South African Wave Energy Resource Data

A Case Study

May 2013

Dr. J. R. Joubert
Prof. J.L. van Niekerk

Centre for Renewable and Sustainable Energy Studies

Faculty of Engineeri kulteit Ingenieurswese

Private Bag / Privaat Sak X1•Matieland, 7602 • South Africa / Suid-Afrika,
Tel: +27 (0) 21 808 4069•Fax / Faks: +27 (0) 21 808 4277
crses@sun.ac.za
http://www.sun.ac.za/crses

Summary

An assessment of the South African wave energy resource was conducted through the analysis of measured and modelled wave data. Wave data recorded at wave measuring stations, representative of the various coastal zones of South Africa, was evaluated and it was found that the southwest coast has the highest wave power resource with a median value of wave power of approximately 26 kW/m. A detailed assessment of the spatial distribution of wave power off the southwest coast was conducted and it was found that the average deep-sea resource ranges from 33 kW/m to 41 kW/m. Results of a detailed assessment of the wave power resource for Table Bay on the southwest coast were presented as an example case study. The study focussed on Granger Bay as a possible deployment site for a shore based wave energy converter. A wave energy focal point was identified just north of Robben Island.

The conclusion from the study is that South Africa does have a significant wave energy resource along the southwest coast that could be exploited as a source of renewable energy. It is recommended that spatial distribution maps of wave power be generated for a larger section of the South African coast. This will assist developers of wave energy technology and projects to identify the best suited locations for the deployment of their devices.

Contents

List of Tables

List of Figures

1 Introduction

1.1 Background to the project

The Centre for Renewable and Sustainable Energy Studies (CRSES) was approached by the South African National Energy Development Institute (SANEDI) to conduct a detailed assessment of the available data on the South African wave power resource, including an example wave energy resource assessment. This has been completed and reported on in a separate project report. Accurate and reliable wave energy resource data is pivotal to the development of an ocean wave energy industry in South Africa. Technology and project developers can identify locations best suited for the deployment of their devices using detailed maps of the spatial distribution of wave power along the coast. This project follows on with an example of a resource analysis and assessment of a specific area and site in the Western Cape.

1.2 Project objective

The main objective of this study is to deliver a detailed description of how to conduct a wave energy resource analysis and assessment along the South African coast, with specific focus on the most energetic coastal zone in the Western Cape. In order to achieve this objective the resource evaluation was divided into three main sections:

1.2.1 Identification of the most energetic coastal region based on recorded wave data

Wave data recorded at wave measuring stations representative of the various coastal zones of South Africa was analysed to identify the most energetic coastal region.

1.2.2 Development of a numerical wave model for the identified coastal region

A numerical wave modelling procedure was developed to simulate wave propagation from deep sea into the identified coastal region. Output from the numerical wave model was used to produce spatial distribution maps of wave power.

1.2.3 Application of the numerical wave model to a selected bay in the identified coastal region

The numerical wave modelling procedure mentioned in § (section) 1.2.2 was employed to generate high resolution spatial distribution maps of wave power for a selected bay, as an example case study in the identified coastal region.

1.3 Methodology

A wave power calculation procedure based on relevant wave theory was discussed and employed to derive the available wave power from measured and modelled wave data. Various statistical parameters of wave power at the recording stations were determined and used to identify the South African coastal zone with the greatest resource. Once identified, a numerical wave modelling procedure using a spectral wave model was employed to transfer offshore wave data. The findings of this report are based on the research conducted by Joubert (2008) and Joubert (2013).

2 Global distribution of wave power and the South African meteorology

2.1 Global distribution of wave power

The world's oceans provide an abundant resource of, as yet, unutilised wave energy. Mørk et al. (2010) have estimated that the global wave energy potential at present stands at approximately 3.7 terawatt (TW) - 75% greater than the total global installed capacity in 2009 (International Energy Agency, 2011). Wave energy is in essence a concentrated form of solar energy. Winds, generated by the differential heating of the Earth's atmosphere, blow over large oceanic areas, transferring its energy to form water waves. The amount of energy transferred and the size of the resulting waves depends on the wind speed, the length of time it blows, and the distance over which it blows, (the 'fetch').

Within or close-to the wave generation area, storm waves known as the 'seas', exhibit a very irregular pattern, and continue to travel in the direction of their formation, even after the wind changes direction or subsides. In deep water, waves can travel out of the storm areas (wind fields) with a minimal loss of energy, and progressively becoming regular, smooth waves known as 'swells', which can persist for great distances (i.e. tens of thousands of kilometres) from the origin.

Therefore, coastlines exposed to the prevailing wind direction and long fetches will have the most energetic wave climate, e.g. northwest coast of North America, southwest coast of South America, Europe, Africa, Australia and New Zealand, as presented in Figure 2-1.

Figure 2-1 shows that the highest wave climates, with annual average power levels between 20 kW/m to 60 kW/m or higher, are found in the temperate zones (30º to 60º north and south latitude) where strong storms occur. However, significant wave climates are still found within ± 30º latitude where regular trade winds blow; the lower power levels being compensated by the smaller wave power variability. South Africa has a world-class wave power resource due to the country's location within the high wave power region, as shown Figure 2-1. This substantial resource can be attributed to its prevailing meteorology conditions.

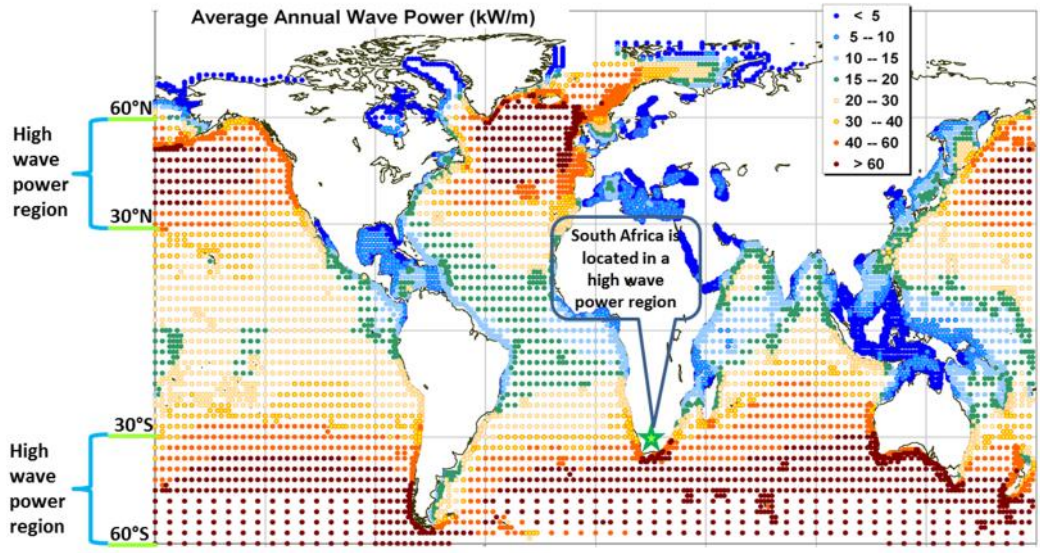

Figure 2-1: Global distribution of mean annual average wave power (kW/m) in deep water (Waves data/OCEANOR/ECMWF)

2.2 South African meteorology

Rossouw (1989) gives a very thorough and concise description of the South African meteorology in his PhD thesis as follows:

> The wind and therefore the wave regime in the South Atlantic and South Indian oceans are influenced by a number of dominant meteorological features. Heated air, which rises in the tropics near the equator, moves southwards and descends in the vicinity of the 30°S to form the so-called Hadley cell. This descending air causes two semi-permanent high-pressure systems, the South Atlantic high and the South Indian high, with the air moving in an anti-clockwise rotation around the centre of the high-pressure system. South of the Hadley cell the air sinks and moves towards the poles creating prevailing westerly winds known as the Ferrel westerlies which spiral eastwards around the globe. Disturbed air in the Ferrel westerlies creates the low-pressure systems of the South Atlantic. Once formed, these low pressure systems moves from west to east within the Ferrel westerly wind system. It is the passage of these depressions with their associated cold fronts and wind fields that are the main cause of ocean waves approaching the South African coastline, shown in Figure 2-2.
>
> These low-pressure systems pass the southern tip of Africa at an approximate frequency of 3 to 5 days. In winter the southern tip of the African continent frequently intersects the path of these depressions. In summer the path of these systems shift further south and the depressions mostly pass south of the continent. More severe wave conditions can therefore be expected to occur more frequently in winter along the southern Cape coast than in summer. The occasional northerly excursion of a cold front does however occur in summer resulting in occasional high waves along this coast during this season as well.
>
> On the southwest coast the wind direction during the passing of these cold fronts (i.e. low pressure systems) normally swings from northwest through southwest to southeast as it passes the southern tip of the African continent. The South African west and south coasts are the most exposed coastal regions to the waves generated by the easterly movement of these low pressure systems.

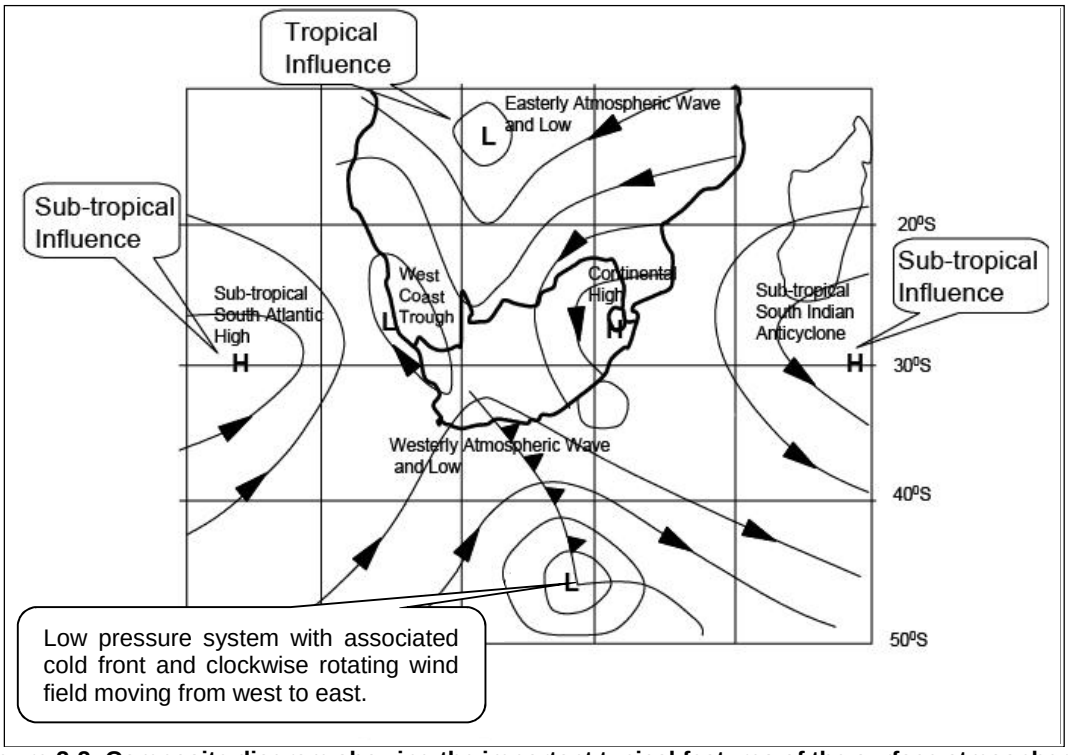

Figure 2-2: Composite diagram showing the important typical features of the surface atmospheric circulation over South Africa (Joubert, 2008).

From Rossouw's description of South Africa's meteorological conditions, one would expect that the west and south coasts would have the greatest wave power resource. In order to quantify this resource, a wave power calculation procedure based on relevant wave theory, is required. This is discussed in the following section.

3 Wave power calculation procedure

3.1 Linear wave theory

Linear, first-order or Airy wave theory (Airy, 1845) has been the basic theory to describe small-amplitude surface gravity waves for about 150 years. The small-amplitude approximation implies that the amplitude of a linear wave is small in comparison to its wavelength and the water depth. Linear theory is based on various assumptions - one of which includes that the motion of water particles is irrotational (particles do not rotate about their own axes). This allows the use of a mathematical function called the velocity potential equation to describe particle velocity in the water. The velocity potential equation and its stream functions can be solved using the equation of Laplace and Bernoulli in combination with suitable boundary conditions as presented by Holthuijsen (2007).

A simple harmonic wave is best described in terms of its parameters such as wavelength, L (horizontal distance between two successive wave troughs or crests), wave period, T (time it takes a wavelength to pass a given point), wave height, H (vertical distance between the trough and succeeding crest) and water depth, d (vertical distance from the seafloor to still water level (SWL)). These parameters are presented for a progressive linear wave in terms of its phase (θ) in Figure 3-1.

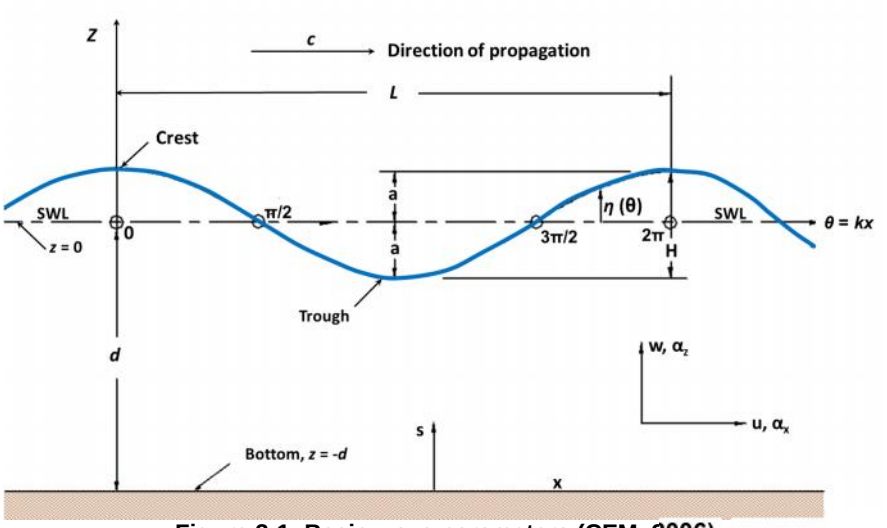

Figure 3-1: Basic wave parameters (CEM, 2006)

Other important wave parameters include the wave number $k = 2\pi/L$ and the angular or radian frequency $\omega = 2\pi/T$.

Surface elevation

The surface elevation, relative to SWL, of a sinusoidal wave as a function of time *t* and horizontal distance *x* can be described as:

$$\eta = \frac{H}{2}\cos\left(\frac{2\pi x}{L} - \frac{2\pi t}{T}\right) = \frac{H}{2}\cos(kx - \omega t) \qquad (1)$$

Particle velocities

Using the surface elevation and velocity potential equation, the horizontal-, *u*, and vertical-, *w*, component of the fluid velocity can be shown to be:

$$u = \frac{H}{2}\frac{gk}{\omega}\frac{\cosh k(d+z)}{\cosh kd}\cos(kx - \omega t) \qquad (2)$$

$$w = \frac{H}{2}\frac{gk}{\omega}\frac{\sinh k(d+z)}{\cosh kd}\sin(kx - \omega t) \qquad (3)$$

Wavelength

The wavelength (*L*) of a regular wave in any water depth is defined as:

$$L = \frac{gT^2}{2\pi}\tanh\left(\frac{2\pi d}{L}\right) \qquad (4)$$

Waves can be classified according to the relative depth (*d*/*L*) criteria. Where:

- Deep water $d/L > ½$
- Transitional depth $1/20 < d/L < ½$
- Shallow water $d/L < 1/20$

Celerity

The propagation speed of an individual regular wave is called the wave celerity or phase velocity, as defined by:

$$C = \frac{L}{T} = \frac{gT}{2®}\tanh(2®d/L) \quad (5)$$

Group velocity

Waves mainly travel in groups from the same direction as a collection of sinusoids with different periods. This is an important concept, because it directly determines the rate at which wave energy propagates in space and time. The propagation velocity of the wave group is called the group velocity (C_g) and is defined as:

$$C_g = \frac{1}{2}\left[1 + \frac{4®d/L}{\sinh(4®d/L)}\right]C \quad (6)$$

Specific energy

The total energy of a progressive, linear wave is the sum of its kinetic and potential energy. The kinetic energy is associated with the water particle velocities and the potential energy is due to the absolute elevation of the fluid mass above and below the SWL. The total energy is given by:

$$E = E_k + E_p = \int_x^{x+L}\int_{-d}^{¦} \circ \frac{u^2 + w^2}{2} dz\, dx + \int_x^{x+L} \circ g\left[\frac{(¦ + d)^2}{2} - \frac{d^2}{2}\right] dx \quad (7)$$

where the subscript *k* and *p* refer to the kinetic and potential energy. After integration it can be seen that the kinetic and potential energy components are equal, provided that the potential energy is relative to SWL and that the waves propagate in the same direction. The total average wave energy per surface area, known as the specific energy or energy density is given by:

$$\overline{E} = \frac{\circ gH^2}{8} \quad (8)$$

Refer to Joubert (2008) for the derivation of Equation (8) from first principles.

Wave power

The rate at which wave energy is transmitted through a vertical plane perpendicular to the direction of the wave advance is known as the wave energy flux or wave power. This is given by:

$$\overline{P} = \frac{1}{T}\int_t^{t+r}\int_{-d}^{¦} pu\, dz\, dt \quad (9)$$

where *p* is the gauge pressure, *t* and *r* are the start and end time respectively.
After integration:

$$\overline{P} = \overline{E}C_g \quad (10)$$

If a vertical plane is taken at an angle other than perpendicular to the wave direction, then $\overline{P} = EC_g sin\theta$, where θ is the angle between the plane over which the energy is transmitted and the wave direction.

To summarise: the total incident wave power per unit width of a linear wave at any water depth is given by:

$$\overline{P} = \frac{°gH^2}{8}\frac{1}{2}\left[1+\frac{4®d/L}{\sinh(4®d/L)}\right]\frac{gT}{2®}\tanh(2®d/L) \qquad (11)$$

From Equation (11), it can be seen that wave power is a function of *H*, *T* and *d*.

3.2 Spectral analysis

The wave theory discussed thus far has mainly been concerned with monochromatic waves which are nearly sinusoidal with a constant height, period and direction. However, real sea states are randomly distributed, irregular waves that are best described statistically. An example of a typical measured wave record is presented in the bottom left-hand corner of Figure 3-2(a).

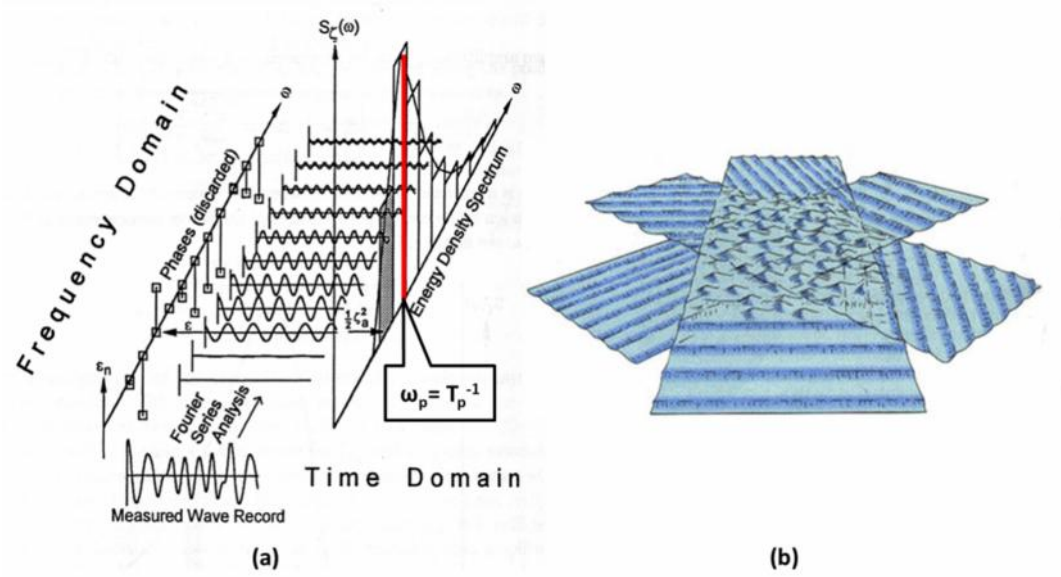

Figure 3-2: (a) Irregular sea state in the time and frequency domain. (b) Directional components of real sea states.

Figure 3-2(a) further shows that the randomly distributed surface elevation of the measured record can be deconstructed with Fourier series analysis into a collection of linear wave components, each with its own unique height and period. The amplitude and frequency of each linear component is used to produce a distribution of wave energy density as a function of frequency called a 1D or frequency spectrum ($E(f)$).

The inverse of the frequency at which the maximum energy density occurs is known as the peak wave period (T_p) of the record, an important parameter in coastal engineering applications. Another key wave parameter is the significant wave height (H_s). H_s or $H_{1/3}$ was traditionally defined as the average wave height of the highest third wave heights in a record. H_s can also be derived from the variance of the spectrum (m_0, zeroth-moment), and is then denoted as H_{m0}. It is generally assumed that $H_s \approx H_{m0}$ therefore:

$$H_s \approx H_{m0} = 4\sqrt{m_0} = \sqrt{\int_0^\infty E(f)df} \quad (12)$$

Where $m_i = \int_0^\infty f^i E(f)df$ is the i^{th} moment of the spectral distribution.

The root-mean-square wave height (H_{RMS}) has been found to best represent the equivalent energy density of an irregular wave record and can be derived from:

$$H_{RMS} = \frac{H_s}{\sqrt{2}} \quad (13)$$

In a similar way, the representative wave period containing the same energy as the irregular wave record is known as the energy period, T_e which is defined as:

$$T_e = \frac{m_{-1}}{m_0} \quad (14)$$

From Equation (14) it is clear that T_e is dependent on the energy density spectrum. It is often difficult to accurately recreate a spectrum from only its measured wave parameters and it is therefore necessary to assume a linear relationship between T_e and T_p (Cornett, 2008) such as:

$$T_e = \sim T_p \quad (15)$$

The shape of a 1D spectrum is generally prescribed in terms of its peak-enhancement factor (γ). Analysis of measured wave spectra off the South African southwest coast indicated that the average γ-value was approximately 1.5 which gives an α value of 0.877. This is considered to be a conservative value of α and was used in the resource assessment of this study.

Typical spectra shapes and peak-enhancement factor

Two of the most common empirical spectral shapes are that of Pierson-Moskowitz (PM) and JONSWAP, as shown in Figure 3-3(a). As mentioned in the previous section, the spectrum shape is described in terms of its peak-enhancement factor (γ). The value of γ is defined as the ratio of the maximum energy density of the JONSWAP and PM spectrum. A PM spectrum is therefore a JONSWAP distribution with a γ-value of 1.

The PM spectrum describes a wave-field that has reached equilibrium for a given wind speed, i.e. no more wind energy is transferred to the wave-field and it is therefore a fully developed sea. It assumes that both the fetch and wind duration is infinite. It has a low γ-value of 1 indicating that the energy density is spread over a large range of frequencies around the peak frequency. The JONSWAP on the other hand has a high, narrow peak around the maximum energy density. JONSWAP is fetch-limited.

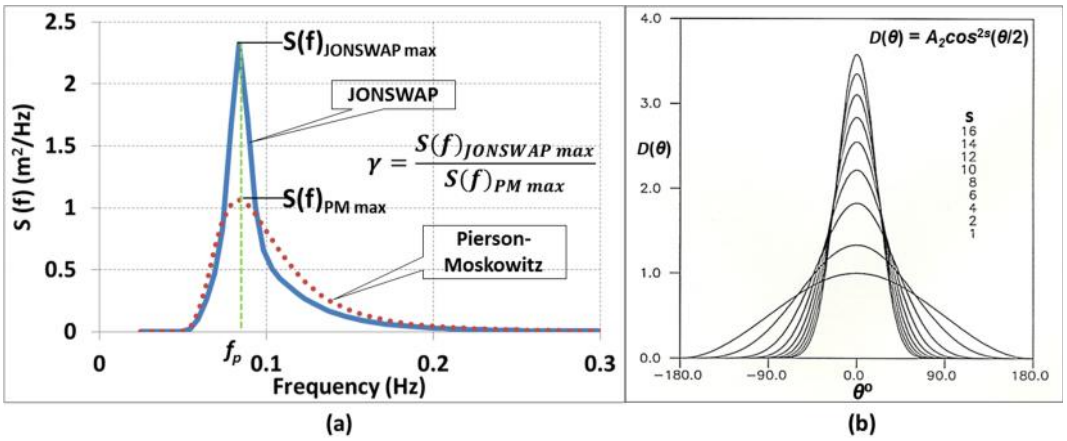

Figure 3-3: (a) 1D energy density spectrum. (b) Directional energy distribution

Two dimensional (2D) wave energy density spectrum

Each sinusoid of an irregular sea state has a propagation direction as shown in Figure 3-2(b). Energy density is therefore also a function of direction. Wave energy density as a function of direction and frequency is known as a 2D spectrum $E(f, \theta)$ (refer to Figure 3-4 for an example 2D spectrum). A model for directional distribution is:

$$D(\theta) = A_2 \cos^{2s}\left(\frac{\theta}{2}\right) \text{ for } -180° < \theta \leq 180° \qquad \textbf{(16)}$$

where $D(\theta)$ is the normalised distribution of the wave energy density over directions at one frequency, $A_2 = \Gamma(s+1)/\left[\Gamma\left(s+\frac{1}{2}\right)2\sqrt{\pi}\right]$ and s controls the width of the distribution. Γ(.) in the A_2 equation above is the gamma function. The direction distribution is presented in Figure 3-3(b) for different s-values. For this study however, the generalised $\cos^m\theta$ model was used, where m controls the width of the distribution.

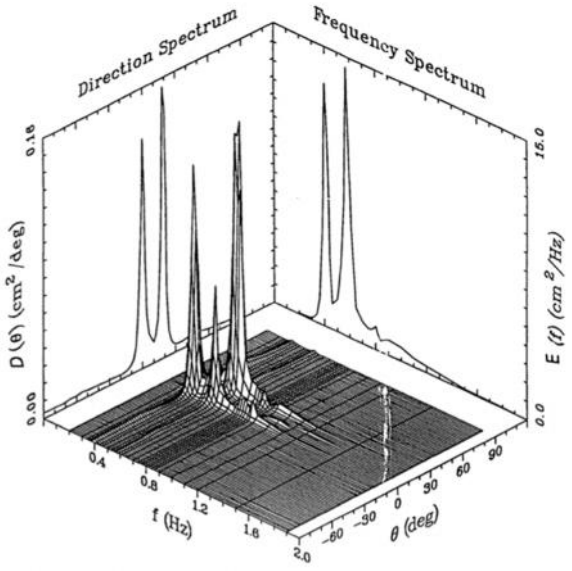

Figure 3-4: Example of 2D spectrum (CEM, 2006)

4 Measured wave data analysis

Wave data recorded at five wave measuring stations, operated by CSIR on the behalf of Portnet, was analysed in this study to determine the most energetic coastal zone of South Africa. The wave data of these stations was deemed representative of the various coastal regions of the country which include the west, southwest, south and east coast respectively. Refer to Figure 4-1 that shows the relative locations of the stations.

Figure 4-1: Distribution of wave recording stations along the South African coast (Google Earth™)

A detailed description of the stations and its wave data is presented in Table 4-1.

Table 4-1: Relevant information of wave recording stations

Recording station	Lat Long coordinates	Distance offshore (km)	Water depth (m)	Description of data	Recording period	% coverage	Wave recorder
Port Nolloth	29° 46.8'S 16° 46'E	30	100	3 Hourly H_{m0} and T_p	1987/04/08 to 1996/08/31	63%	Waverider
Slangkop	34° 7.6'S 18° 10.6'E	13	170	6 Hourly H_{m0} and T_p	1978/10/03 to 1993/06/12	72%	Waverider
Cape point	34° 12.2'S 18° 17.2'E	7	70	3 Hourly H_{m0} and T_p	2000/07/01 to 2006/06/30	92%	Waverider
FA platform	34° 58.2'S 22° 10.2'E	72.5	113	1 Hourly H_{m0}, T_z and H_{max}	1998/01/01 to 2003/12/31	97%	Radar
Durban	29° 59.2'S 30° 59.9'E	2.3	42	3 Hourly H_{m0} and T_p	1992/08/11 to 2001/10/31	69%	Waverider

As waves propagate from deep sea to shore the bathymetry, i.e. the water depth, greatly influences the resulting nearshore wave climate. Therefore the position of the wave recoding stations relative to the continental shelf affects its exposure. The continental shelf is

presented as the light blue area in Figure 4-1 with its edge at approximately the 200 m depth contour, as shown in Figure 4-2. The Slangkop, Cape Point and Durban wave recording stations are located in a zone where the shelf is relatively narrow in comparison with the wider area at the recording stations of Port Nolloth and FA platform.

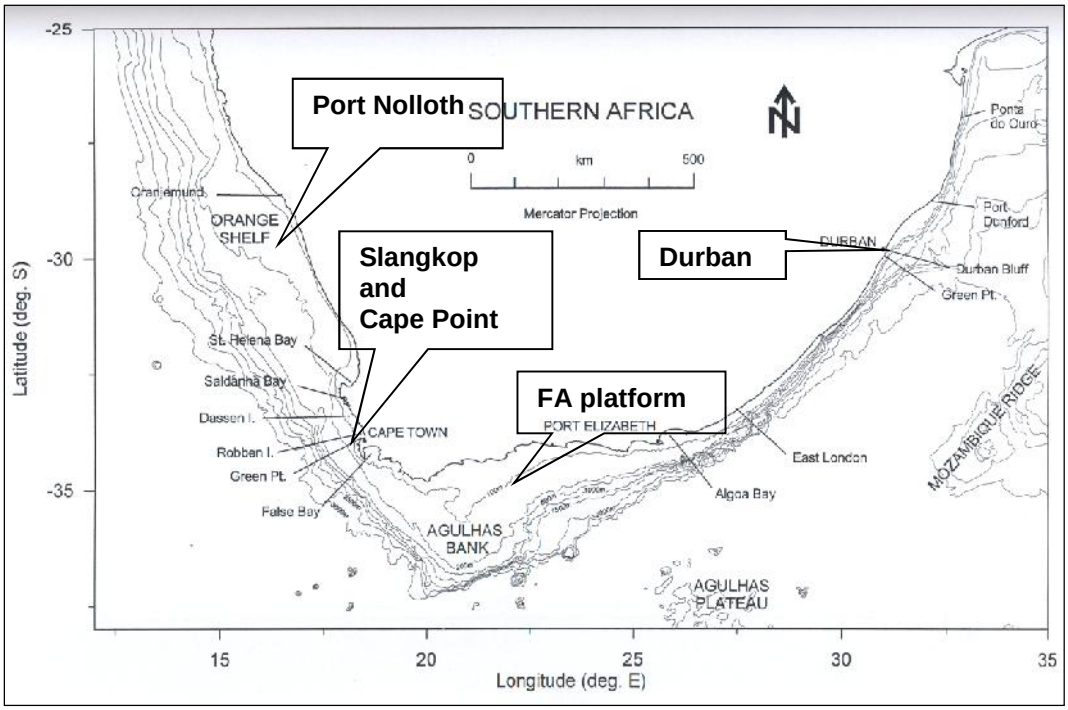

Figure 4-2: Contours of the Southern African seabed to 3000 m depth

A brief description of the wave recording stations considered is presented below.

4.1 Port Nolloth

The Port Nolloth wave data represents the wave power associated with the South African west coast. Waves generated by the extra-tropical cyclone systems (low pressure systems) in the southern ocean (between approximately the 40° and 60° latitude zone) approach the South African west coast, predominantly from the south-westerly sector. See Chapter 2.2 for a description of the South African meteorology. It is expected that wave heights and consequent wave power will decline the further north the waves travel from the storm generation zone.

4.2 Slangkop

The Slangkop Waverider buoy was situated about 13 km directly west of Kommetjie (see Figure 4-3) during the period of 1978 to 1993. The radio signal sent from this buoy was received at the Slangkop lighthouse. In 1994 the Slangkop wave recording station was relocated to the present Cape Point recording station. Slangkop and Cape Point are the most south-westerly located stations and the first stations to receive the wave power propagating from the dominant south-westerly direction. The water depth at the Slangkop recording station was 170 m only 13 km from shore, indicating that the continental shelf has a steep gradient in this region (see Figure 4-2).

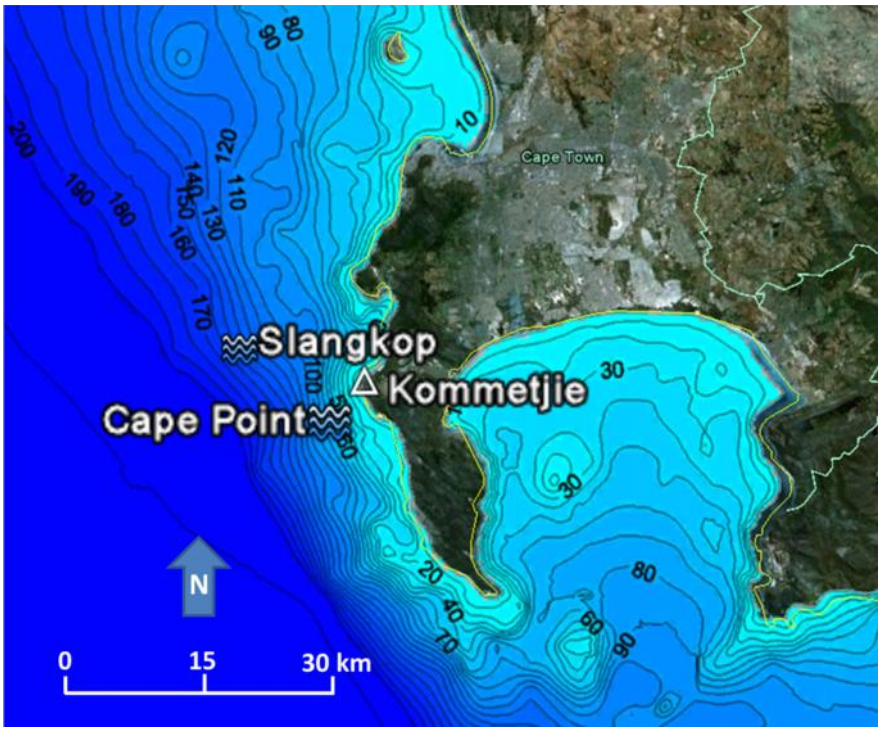

Figure 4-3: Locations of Slangkop and Cape Point wave recording stations

4.3 Cape Point

The Waverider buoy at the Cape Point recording station is situated in water depth of 70 m approximately 7 km southwest of Kommetjie. It is expected that the shallower water depth at Cape Point recording station will expose it to lower wave power levels compared to the Slangkop station due to the increased losses caused by bottom friction. Local bathymetric conditions could however, also focus wave power at the Cape Point station for specific wave conditions, which could increase its wave power exposure compared to Slangkop for those specific wave conditions. A direct comparison between these two stations is not possible since there is no overlapping in their recording periods, but it is expected that the two stations will have similar wave power conditions due to their close proximity.

4.4 FA platform

The FA platform is located approximately 73 km offshore at a depth of 113m. The platform produces natural gas from substrata below the seabed. The natural gas is pumped via a subsea pipeline to the shore-based refinery operated by PetroSA, near Mossel Bay.


Figure 4-4: Arial view of the FA platform (http://www.petrosa.co.za 27 March 2013)

4.5 Durban

The recorded wave climate at the Durban wave recording station represents the expected wave power along the east and south coast of South Africa. The Durban station is not as exposed to wave power from the southwest as the other recording stations. It does however

experience wave power generated from tropical storms in the east. The Waverider buoy at the Durban recording station is located offshore of the Durban oil refinery near the old Durban Airport (i.e Louis Botha Airport).

4.6 Wave height analysis

Equation 11 shows that wave power is proportional to the wave height squared. An analysis of the wave height distribution of the various stations will therefore provide a general indication of the expected wave power conditions at each station along the coast. Wave heights are also important design parameters from a wave energy conversion and survivability design perspective. The probability of exceedance curves of H_{m0} is presented for all the stations in Figure 4-5. Figure 4-5 shows that FA platform has the greatest H_{m0} values with the highest probabilities of exceedance, followed by Slangkop, Cape Point, Port Nolloth and Durban.

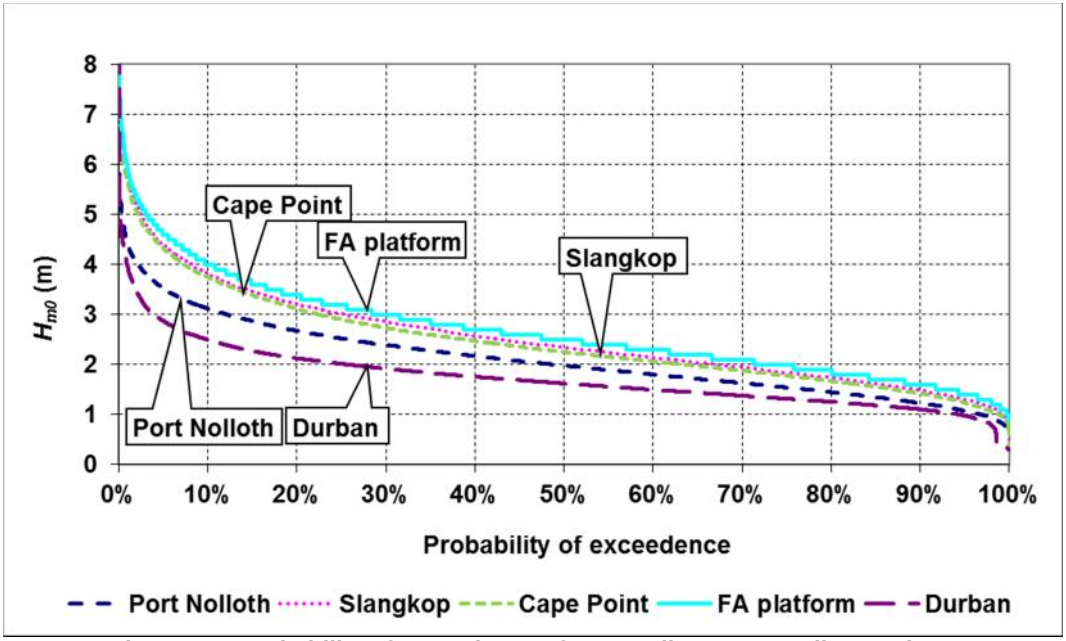

Figure 4-5: Probability of exceedance of H_{m0} at all wave recording stations

The frequency of occurrence of H_{m0} for the various stations, presented in Figure 4-6, shows that the most frequently occurring wave height for FA platform, Slangkop and Cape Point is approximately 3 m which occurs 40% of the data sets. Port Nolloth and Durban's most frequently occurring value of H_{m0} is approximately 2 m which occurs 50% and 70% respectively. Port Nolloth does however also experience greater wave heights. From this wave height analysis, the FA platform is expected to have the greatest wave power resource of all the stations.

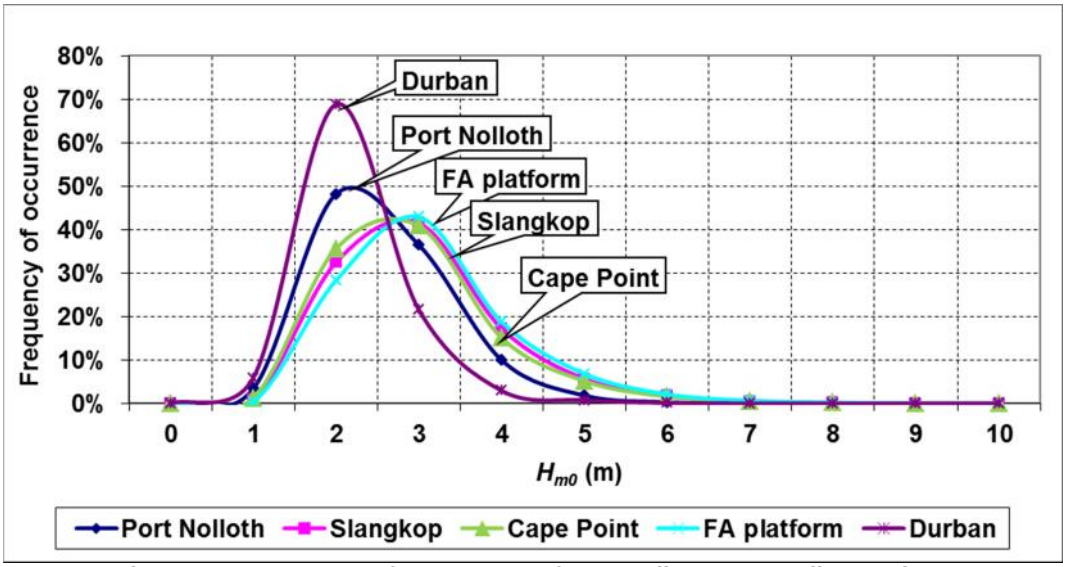

Figure 4-6: Frequency of occurrence of H_{m0} at all wave recording stations

Wave height is a very important design parameter for wave energy devices from a survivability perspective and therefore the maximum wave heights recorded at each station and the resulting hundred year design storm wave height, as derived by MacHutchon (2006), are presented in Table 4-2.

Table 4-2: Design wave heights based on measured wave data (MacHutchon, 2006)

Stations	Max H_{m0} recorded (m)	$H_{1/100}$ (m)
Port Nolloth	6.4	9.2
Slangkop	10.8	11.8
Cape Point	10.0	11.8
FA platform	10.7	12.0
Durban	6.3	7.8

4.7 Wave period analysis

Wave power is linearly dependent on wave period, and thus the wave period parameter will provide another indication of the expected energy resource. The response of wave energy devices is highly dependent on the prevailing wave period conditions. Devices are typically designed for resonant response, i.e. when the natural period of the system matches the incident wave period. For optimal performance the device response is tuned to the prevailing wave periods. Wave period also determines the wavelength of the incident waves which is another important design consideration.

The frequency of occurrence of wave periods recorded at the various stations, presented in Figure 4-7, shows that the most frequently occurring peak wave period at Port Nolloth, Slangkop and Cape Point is approximately 12 s, while the more eastern stations of the FA platform and Durban is approximately 9 s. This lower T_p value at the platform is expected to reduce its wave power distribution compared to Slangkop- and Cape Point recording stations. The typical wavelength, as a function of wave period and water depth, is 223 m, 225 m, 217 m, 126 m and 123 m for Port Nolloth, Slangkop, Cape Point, FA platform and Durban recording stations respectively.

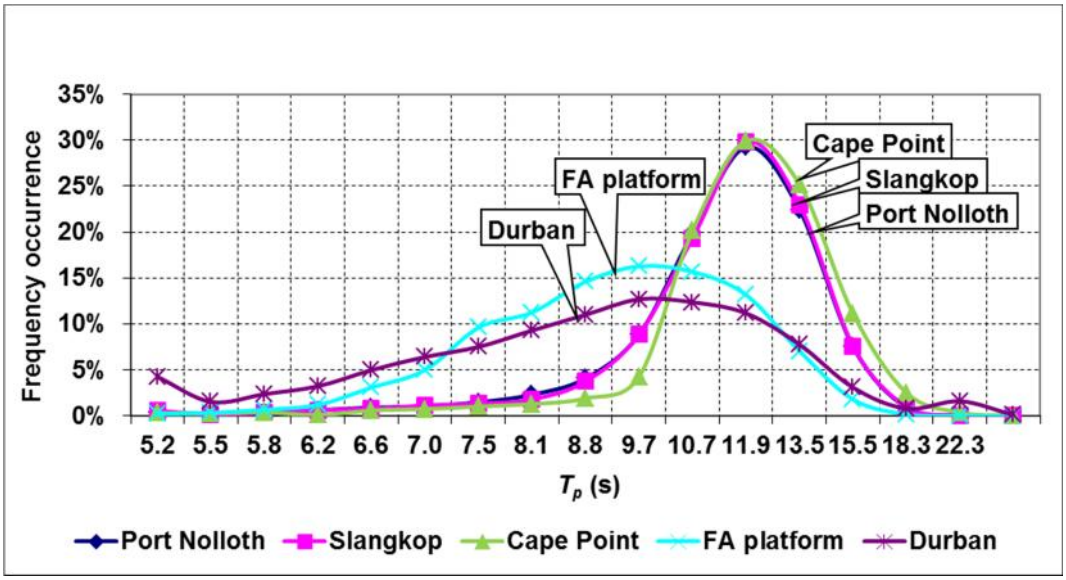

Figure 4-7: Frequency of occurrence of T_p at all wave recording stations

Rossouw (1989) recommends design peak wave periods as prescribed by Del Norske Veritas (1977) of:

$$3.6\sqrt{H_{m0}} < T_p < 5.5\sqrt{H_{m0}}$$

Rossouw (1989) found that this relationship between T_p and H_{m0} agrees favourably with measured wave data off South Africa's coast.

Wave power as a function of various wave period parameters, including T_p, T_e and T_m (mean wave period), was evaluated to demonstrate its sensitivity to these parameters. Results of the wave power calculations, using Equation 11, are presented in Table 4-3 for three wave heights at the Slangkop recording station. T_p produces the greatest wave power, while T_e and T_m result in more conservative estimates. The value of wave power generated by T_e is 20% greater than that of T_m. Various sources in the literature recommend the use of T_e in wave power calculations; refer to Payne (2008) and Pitt (2005).

Table 4-3: Wave power as a function of T_p, T_e and T_m

H_{m0} (m)	P (kW/m) for T_p = 12 s	P (kW/m) for T_e = 10.44 s	P (kW/m) for T_m = 8.4 s
2	23.58	20.49	16.48
4	94.32	81.96	65.94
6	212.21	184.40	148.36

This concludes the discussion of wave parameters relevant to wave power. In the following section a comparison the wave power distribution at the various stations is presented.

4.8 Wave power analysis

4.8.1 Probability of exceedance and frequency of occurrence

The probability of exceedance curves of wave power for all the stations, show that Slangkop and Cape Point have the greatest wave power distribution, followed by FA platform, Port Nolloth and lastly Durban. This is presented in Figure 4-8. For comparative purposes wave power events exceeding 100 kW/m were not included in the analysis.

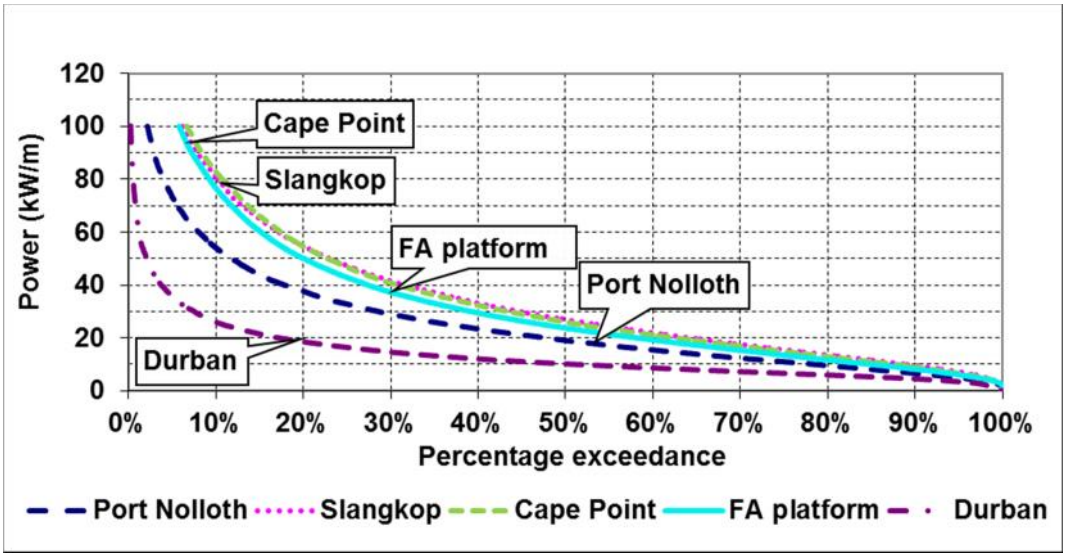

Figure 4-8: Probability of exceedance of wave power at all the wave recording stations

The frequency of occurrence curves of wave power for the various stations, presented in Figure 4-9, shows that Durban has a high occurrence of low wave power events, while the other stations have lower occurrences of high wave power events.

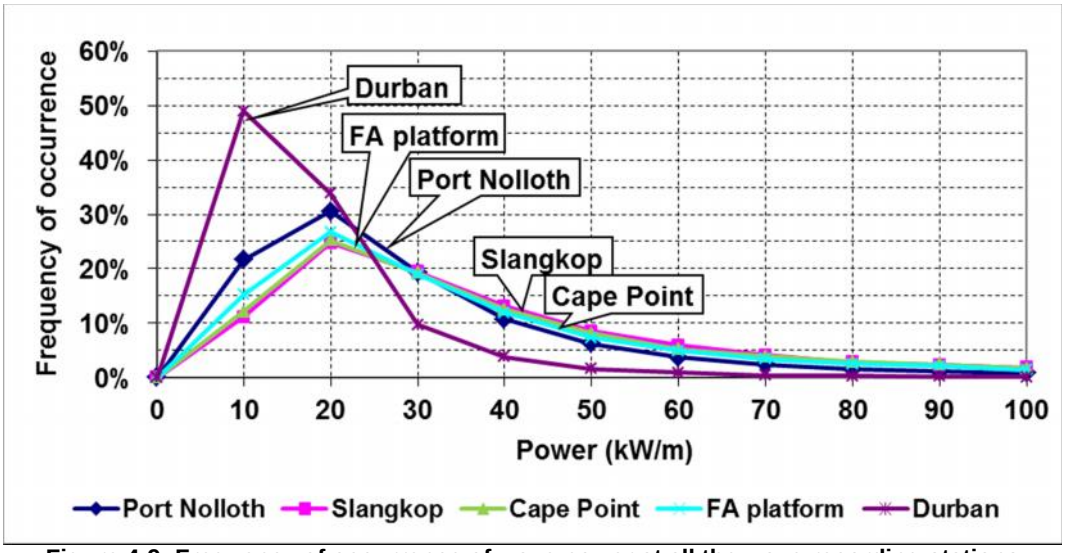

Figure 4-9: Frequency of occurrence of wave power at all the wave recording stations

The 5%, 50% and 90% probability of exceedance of wave power plots for each station are shown in Figure 4-10. These probabilities represent the extreme, average and lowest recorded wave power events. Figure 4-10 shows that Slangkop and Cape Point have the highest mean annual median values of approximately 26 kW/m, followed by FA platform, Port Nolloth and Durban with values of 24 kW/m, 19 kW/m and 10 kW/m respectively.

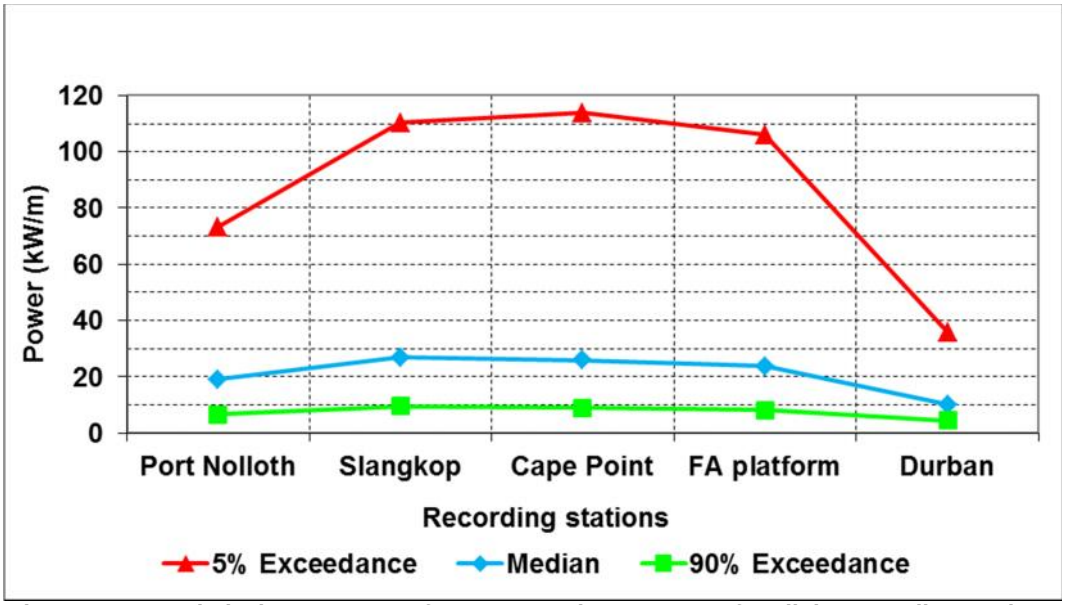

Figure 4-10: Statistical parameters of mean annual wave power for all the recording stations

4.8.2 Mean monthly wave power distribution

The variability of wave power for a typical year is represented as mean monthly median values for all the stations in Figure 4-11. Figure 4-11 shows that, as expected, the winter months of June, July and August are the most energetic followed by the months of autumn, spring and lastly summer. Slangkop and Cape Point again have the highest mean monthly wave power distribution.

The minimum expected mean monthly wave power available is expressed in terms of 90% probability of exceedance in Figure 4-12.

The mean monthly variability of wave power is demonstrated by the standard deviation for each station, in Figure 4-13. Slangkop and Cape Point have the greatest resource, but also the greatest resource variability. Wave energy devices deployed here will therefore have to be able to operate optimally over a wide range of wave conditions. The resource available at Port Nolloth is significantly lower than that of the southwest stations, but presents a more constant, less variable resource.

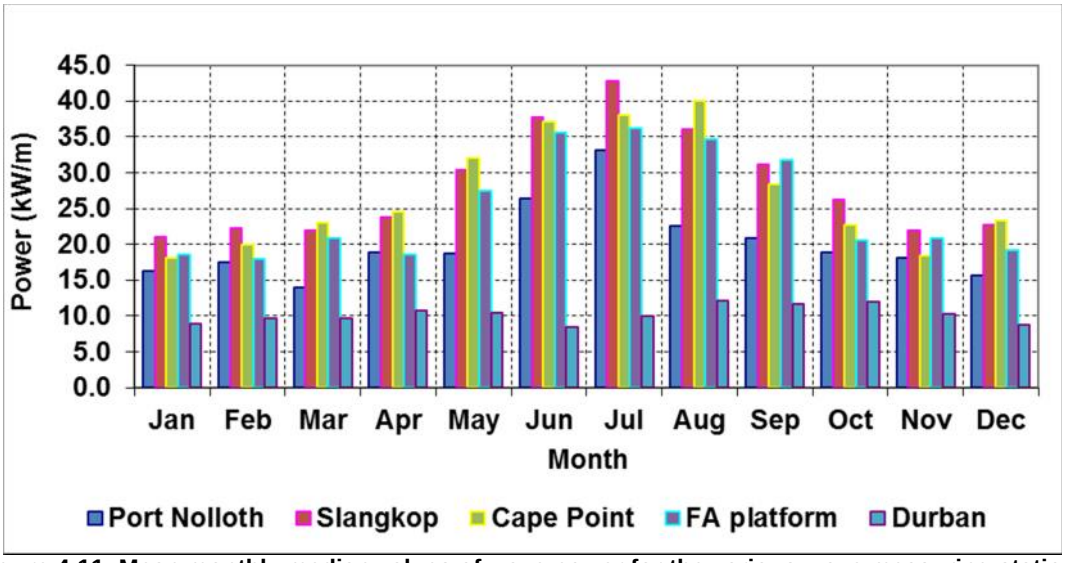

Figure 4-11: Mean monthly median values of wave power for the various wave measuring stations

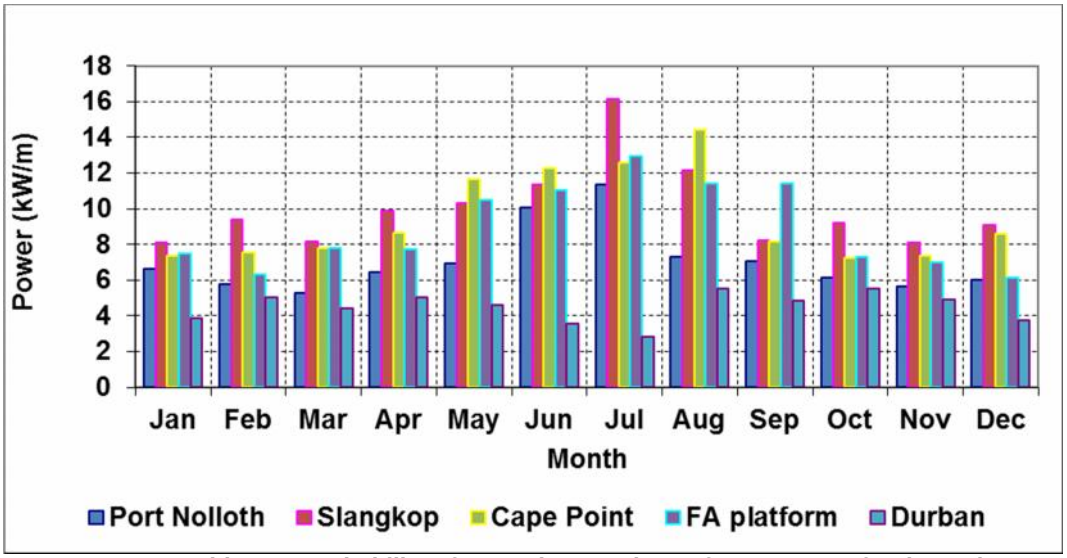

Figure 4-12: Mean monthly 90% probability of exceedance values of wave power for the various stations

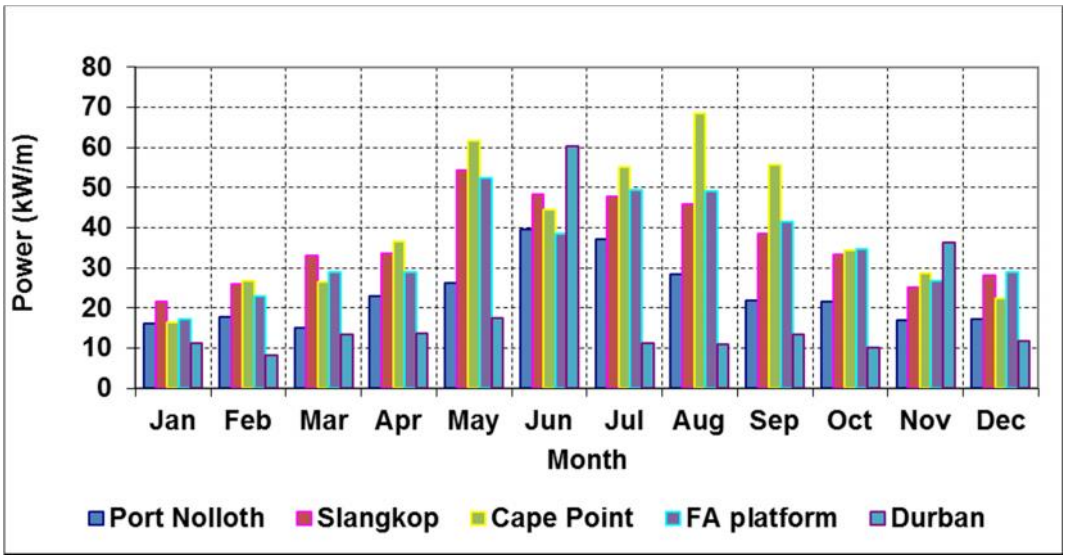

Figure 4-13: Mean monthly standard deviation of wave power for the various stations

4.8.3 Wave energy scatter analysis

An example of a wave energy scatter analysis, as presented by Hagerman and Bedard (2003), was conducted on the recorded wave data of Cape Point. A wave energy scatter diagram is a surface contour graph of the annual wave energy (expressed in megawatthours, MWh) available from each combination of wave height and wave period. The wave energy scatter diagram of Cape Point presented in Figure 4-14 shows that the most frequently occurring and energetic combinations of wave height and wave period range from 2.0 m to 3.0 m and 11 s to 13 s respectively, and produce between 16 MWh to 20 MWh per meter wave crest per year. The total generation potential available from all occurring combinations of wave height and period is 345 MWh per meter wave crest per year. To put this figure into perspective let's assume a 100 m of wave front is captured and converted by a WEC device into electricity at a 30% efficiency. Therefore, the total electricity generated by the WEC will be 10.4 GWh per annum which is comparable to a 1.5 MW wind turbine which generates approximately 6 GWh per annum.

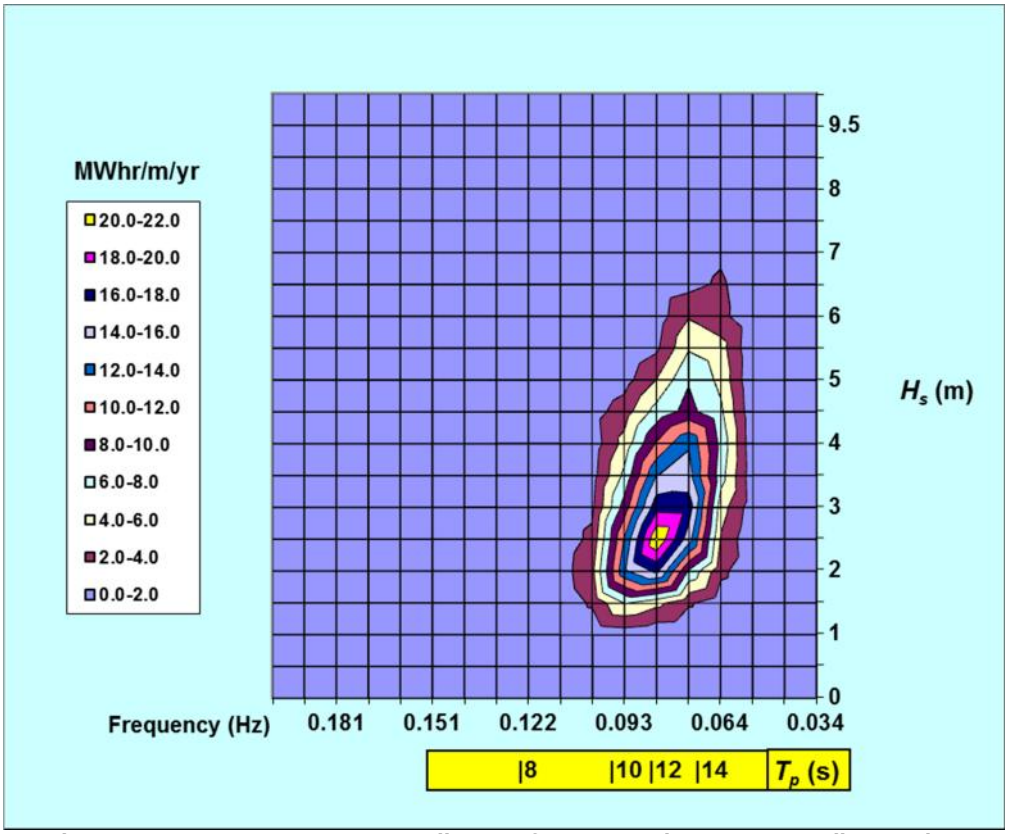

Figure 4-14: Wave energy scatter diagram for Cape Point wave recording station

From this analysis it was concluded that the South African southwest coast has the greatest wave power resource and its spatial distribution was therefore further investigated in the following section.

5 Spatial distribution of wave power off South Africa's most energetic coastal zone

The results of the measured wave data analysis, presented in Chapter 4, provide a general description of the wave power conditions at locations with available wave data. From the analysis it was found that the southwest coast has the greatest wave power resource. The analysis of wave data recorded at the wave recording stations of Slangkop and Cape Point is an indication of the expected wave power exposure of the southwest coastal region. In order to identify locations best suited for wave energy conversion, a detailed description of the spatial wave power distribution of the whole area is required.

This objective is achieved through the numerical simulation of ocean wave propagation over the above-mentioned coastal region. In order to simulate wave transformation from deep water (offshore) to near-shore, deep sea wave data is required as input into the numerical model. The deep-sea input wave data must be at sufficiently deep-water depths at which little or no wave-bottom interaction occurs. The Slangkop and Cape Point recording stations are situated near-shore and their wave data is therefore not considered to be ideally suitable. Global wave models, on the other hand, describe wave conditions at deep-sea locations over the entire globe. Historic output of global wave models (which are normally validated and adjusted if necessary), is known as hindcast wave data and is used in the numerical simulation application of this study.

This investigation quantifies the wave power resource of Cape Point to Elands Bay and is the focus area of this part of the study. The wave power climate of the focus area will be quantified by simulating wave propagation from deep sea (using 10 years of hindcast data) to shore using the SWAN wave model.

5.1 Offshore wave data used in the study

The input offshore wave data used for this spatial distribution of wave power assessment was obtained from the National Center for Environmental Prediction (NCEP). NCEP is a department of the National Oceanic and Atmospheric Administration (NOAA), which is an agency of the United States federal government responsible for monitoring the global climate and environment. NCEP comprises of nine centers, including the Environmental Modelling Center, which develops, improves and monitors data assimilation systems and models of the atmosphere, ocean and coupled system (NCEP Internet team, 2007). NCEP provides operational ocean wave predictions using the wave model Wave Watch III with operational NCEP products as input. Wave Watch III is a third generation wave model developed by NCEP based on the WAM wave model.

Tolman (2006), a developer of WAVEWATCH III, describes the wave model's functionality as follows:

> "WAVEWATCH III solves the spectral action density balance equation for wavenumber-direction spectra. The implicit assumption of this equation is that properties of medium (water depth and current) as well as the wave field itself vary on time and space scales that are much larger than the variation scales of a single wave. A constraint is that the parameterisations of physical processes included in the model do not address conditions where the waves are strongly depth-limited. These two basic assumptions imply that the model can generally by applied on spatial scales (grid increments) larger than 1 to 10 km, and outside the surf zone."
> (NOAA: Marine modelling and analysis branch, 2012)

Considering that the focus of this portion of the study is on the near-shore resource, further numerical wave modelling is required to simulate wave propagation from the deep sea NCEP location to shore. The NCEP global model output is calibrated and validated with buoy data and with European Remote-Sensing Satellites (ERS2) fast-delivery altimeter (measures altitude above a certain datum) and scatterometer (measures scatter from the ocean surface) data. An analysis of the NCEP data is presented in the following section.

5.1.1 Analysis of offshore NCEP wave data

The offshore NCEP wave data used as input to the nearshore wave model is located at 34ºS 17.5ºE, 33ºS 17.5ºE, 32ºS 17.5ºE, 31ºS 17.5ºE and 35ºS 17.5ºE (refer to Figure 5-1). The hindcast wave data set was obtained for February 1997 to September 2006, almost 10 years. The wave data is available in three hourly intervals and each record consists of the date- and time of recording, significant wave height (H_{m0}), peak wave period (T_p), and peak wave direction (D_p). The wave data is a 100% complete set, consisting of 27 992 records. As a quality assurance measure, the NCEP wave parameters at 34ºS 17.5ºE were compared to wave data recorded by the Cape Point wave measuring buoy for the period the two data sets overlap, which was July 2000 to July 2006. It is expected that the NCEP wave heights will be greater than Cape Point's due to the energy losses occurring as waves propagate to the shallower water location.

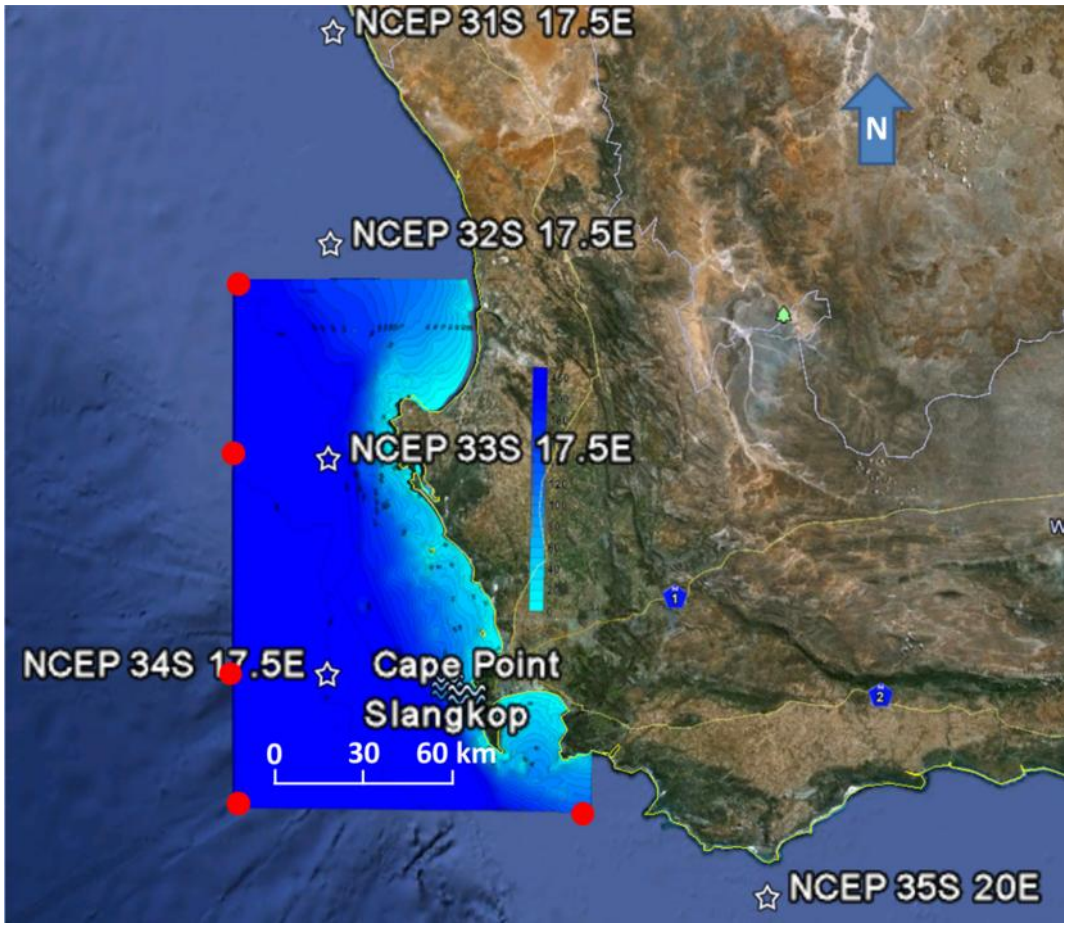

Figure 5-1: Relative location of the offshore NCEP data points to the southwest coastal region, Slangkop and Cape Point wave recording stations. Red circles indicate SWAN input values on the model computational boundary.

The NCEP wave parameters were analysed and compared to Cape Point measured data. The results of the data analysis are presented in the following sections.

5.1.2 Wave height distribution

Wave height is a very important wave parameter not only to determine the available resource, but also for design purposes. It is therefore imperative that the input NCEP wave height data is of an acceptable standard and compares well to the measured wave data of Cape Point.

The probability of exceedance curves of wave height in Figure 5-2(a) show that the NCEP wave heights are on average 0.3 m greater than Cape Point's. This reduction in wave height occurs as waves travel to the shallower water of the Cape Point location, and can be ascribed to energy losses caused by bottom friction. In general the NCEP wave height data has a similar probability of exceedance distribution compared to the Cape Point data and therefore appears to be of acceptable quality.

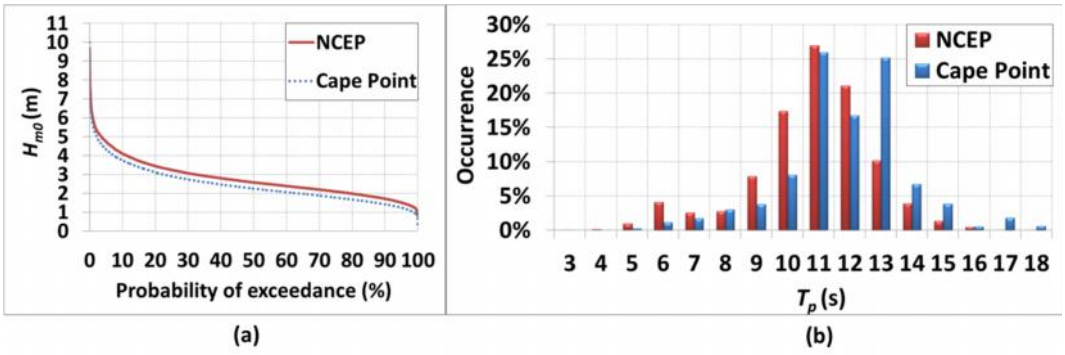

Figure 5-2: (a) Probability of exceedance of wave height at NCEP 34ºS 17.5ºE and measured at Cape Point wave recording station. (b) Frequency of occurrence of wave period at NCEP 34S 17.4E and measured at Cape Point wave recording station July 2000 to July 2006

A comparison of the NCEP and Cape Point wave period data is presented in the next section.

5.1.3 Wave period

The frequency of occurrence of wave period bar graphs for NCEP and Cape Point presented in Figure 5-2(b) show that both data sets' most frequently occurring wave period is 11 s for approximately 25% of the six-year period. In general the Cape Point data contains higher values of wave period occurring more frequently than the NCEP data, indicating that the NCEP data might slightly underestimate the wave period conditions off the South African coast. This could be due to local effects not being included in the NCEP model or the Cape Point buoy's recording frequency bins. In general the frequency of occurrence graphs of the two data sets correlate sufficiently to warrant the use of the NCEP wave period data.

5.1.4 Directional distribution

The CSIR replaced the non-directional buoy at Cape Point with a directional Datawell Waverider in 2001. Unfortunately none of this directional wave data was available for comparison with the NCEP directional data. The frequency of occurrence of NCEP's peak wave direction data plotted on the contour graph in **Error! Reference source not found.** confirms the predominant south-westerly direction of approaching waves as stated by Rossouw (1989).

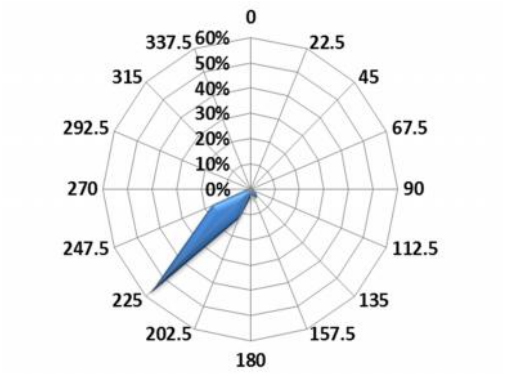

Figure 5-3: Directional wave rose showing the frequency of occurrence of peak wave direction NCEP 34ºS 17.5ºE

The accuracy of the NCEP data and the output of the nearshore wave model will be validated through further comparison with CSIR recorded wave data as presented in §5.5. A discussion of the SWAN wave model used to simulate the propagation of waves from the NCEP offshore locations into southwest coastal zone is presented in the following sections.

5.2 Background of the SWAN wave model

SWAN, an acronym for **S**imulating **WA**ves **N**earshore, is a third-generation wave model used to obtain estimates of wave parameters in coastal areas, lakes and estuaries from given wind, bottom and current conditions according to the user manual of SWAN Cycle III version 40.85. SWAN was developed at the Delft University of Technology and is continuously improved. Unlike most other coastal wave models, SWAN is freely available and open-source. It is described in peer-reviewed literature and is used by more than 250 institutions (Allard and Rogers, 2004). The SWAN model solves spectral action balance equations and accounts for shoaling and refraction (depth and current induced), wave generation due to wind, energy dissipation due to whitecapping, bottom friction and depth-induced wave breaking, as well as nonlinear wave-wave interactions (quadruplets and triads).

5.3 Wave transfer methodology

As stated earlier, the objective of this part of the study was to transfer NCEP's 10 years of wave data from offshore to the focus area to enable the investigation of the spatial distribution of wave power. The most direct way to achieve this would be to do a SWAN simulation for each of the 27 992 NCEP records. Such an operation would have been very computationally intensive, making it impractical.

To simplify the computational effort NCEP wave direction and period data were divided into bins (0 s to 30 s in 2s intervals and 0º to 337.5º in 22.5º intervals) and the variation in wave height on the model boundary and over the computational grid was determined relative to the offshore wave height at NCEP 34ºS 17.5ºE using SWAN. SWAN output includes the variation in wave direction and wave height over the computational area for each offshore wave period and direction combination. The wave height variation, expressed as a percentage of the offshore input wave height at NCEP 34ºS 17.5ºE, is used to determine the wave height in the focus area.

The presented wave modelling procedure is based on the assumption that the wave height variation is relative to an offshore wave height of approximately one. Energy dissipation processes such as bottom friction greatly influence the resulting wave heights in shallow water and are also a function of wave height. In an attempt to determine the sensitivity of wave height variation to the input offshore wave heights, SWAN simulations were conducted for greater offshore wave heights. It was found that the model underestimates dissipation for

larger waves in shallow water. However, the discrepancies are marginal and are shown to not greatly influence the overall accuracy of the model (refer to the model validation in §5.5).

5.4 SWAN input requirements

As mentioned earlier, the main focus of this study is to develop a general description of the expected wave power conditions of the study focus area. Time dependent simulations were deemed unnecessary for this purpose and are more applicable to site specific designs and real time simulations. Similarly, wind and current inputs were also excluded from all simulations. For SWAN to model wave propagation from the input boundary conditions, a computational domain and associated bathymetric grid must be defined.

5.4.1 Computational and bathymetric grid

A uniform, rectangular (regular) computational grid was specified for the SWAN simulation, containing a 166 km by 272 km area of the southwest coastal region, including its 300 km coastline. This area covers approximately 2^0 latitude (32.1^0S to 34.6^0S) and 2^0 longitude (17.2^0E to 19ºE). The grid resolution was set equal to 1 x 1 km^2, which implies 167 and 273 grid lines in the x- and y-directions, respectively. This results in a total of 45 591 grid points (about 50% on land) over the entire grid.

A 1 km x 1 km mesh is considered sufficient for wave energy transfer in deep water, but too coarse in shallower water (i.e. water depths less than approximately 50 m). For the purpose of this study it is considered that the chosen grid spacing is sufficient to achieve the project objective since the main zone of interest was from deep sea to a depth of 50 m. (In water depths shallower than 50 m the chosen grid spacing is relatively coarse and for WEC site specific design in shallower water, a finer nested grid within the chosen 1 km x 1 km grid will be necessary, refer to Chapter 6).

The computational- and bathymetric grid used in the SWAN simulations are presented in Figure 5-1. The bathymetric grid was derived from naval chart SAN 79. The datum of the seabed depths on the SA Naval chart is Chart Datum which is about 1m below Mean Sea Level (MSL). MSL was chosen as the water level for the SWAN analysis, since this is the dominant water level with a tidal range of about 1m above and 1m below MSL.

5.4.2 Boundary conditions

The final requirement for the simulation process is to prescribe the wave conditions on the boundaries of the computational grid. The computational grid shown in Figure 5-1 has three water- (south, west and north) and one land boundaries (east). The coastline in the study area was defined as fully absorbent in SWAN.

The wave fields on the model boundaries were prescribed as energy density spectra defined by shape, directional distribution, significant wave height, peak wave period and peak wave direction. A discussion of these parameters follows.

Peak enhancement factor (γ)

The shape of the energy density spectrum was prescribed in terms of its peak enhancement factor (*γ*). Refer to §3.2 for a detail discussion of spectral shapes. The *γ*-values recorded at the Cape Point measuring station, over a six year period, were analysed to determine the shape of the input energy density spectrum on the model boundary. The *γ*-values were divided into directional bins and a linear relationship between *γ* and wave height and *γ* and wave period was determined. The average *γ*-values as prescribed by the two linear relationships were used as input into the wave model.

Directional spreading (m)
The directional distribution of energy density on the model boundaries was prescribed in terms its directional spreading. Refer to §3.2 for a detail discussion of directional distributions. In order to determine the values for directional spreading best suited for South African wave conditions, spreading values recorded at Cape Point station over a six year period were analysed. A similar analysis to that conducted on the γ-values was done for the measured spreading values. The most probable spreading values as a function of wave height and wave period were determined.

Wave height
As stated in §5.3, SWAN simulations were done to determine the wave height variation of each occurring combination of wave period and wave direction relative to the offshore wave height of NCEP 34ºS 17.5ºE. The variation in wave height as determined by SWAN was expressed as a percentage of the input offshore wave height of NCEP 34ºS 17.5ºE. One year of NCEP wave data, at the various NCEP grid points shown in Figure 5-1, was analysed to determine the variation of wave height as a function of x and y-distance. These functions of wave height variations were used to prescribe the input wave height conditions on the model boundaries (refer to the red circle in Figure 5-1).

Wave period
The wave period input conditions were prescribed in terms of T_p. The T_p range of 0 s to 30 s in 2 s intervals was simulated, encapsulating the entire T_p range of NCEP 34ºS 17.5ºE.

Wave direction
The entire directional spectrum from 0º to 337.5º in 22.5º intervals was simulated.

This concludes the discussion of the input boundary conditions required for SWAN. In the next section the model output is validated through comparison with measured wave data.

5.5 Southwest coast model validation

The accuracy of the model output was investigated by comparing it to the measured data of the Cape Point recording station. The closest model grid point to the Cape Point recording station is located 390m south of the Cape Point station at a depth of 78m compared to 70m water depth at Cape Point. The recording period of the Cape Point recording station and NCEP 34ºS 17.5ºE data overlaps for a six year period from July 2000 to July 2006. Data recorded during this period will be used for comparison purposes.

The mean monthly median values of wave power for Cape Point and the nearest model grid point are presented in Figure 5-4. Figure 5-4 shows that the model overestimates wave power in comparison with the Cape Point data by an average of 10%.

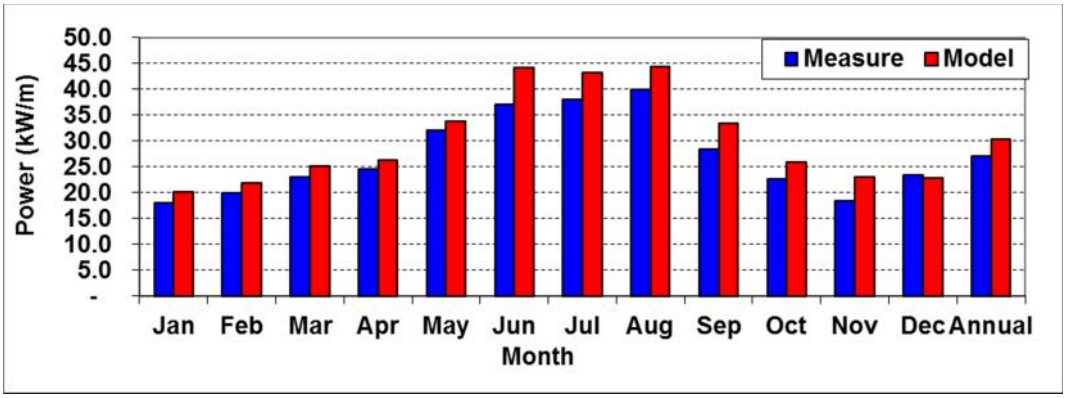

Figure 5-4: Mean monthly median values of wave power at Cape Point and the nearest model grid point for July 2000 to July 2006

The probability of exceedance of wave power as predicted by the model and recorded at Cape Point is presented in Figure 5-5. Figure 5-5 shows that model's probability of exceedance curve closely follows that of the measured data at low (90% to 100%) and high (6% to 15%) wave power events, but again overestimate the resource for the bulk of the data (20% to 80%). In general the model output proved to be of an acceptably accurate standard for the purpose of this study.

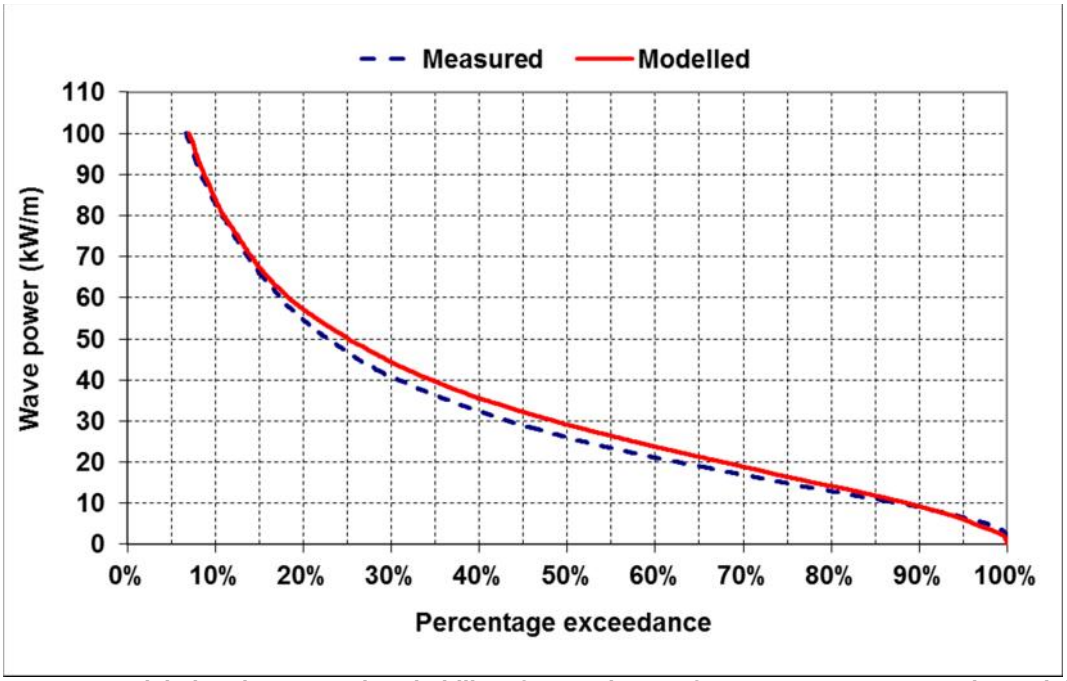

Figure 5-5: Modeled and measured probability of exceedance of wave power at Cape Point and the nearest model grid point for July 2000 to July 2006

5.6 Model output

An example of the model output is presented as the mean annual spatial distribution of average wave power in the study area over a 10 year period shown as a wave power contour map in Figure 5-6. Some important conclusions drawn from Figure 5-6 include:

- The Southern Atlantic Ocean is the main source of wave power in the southwest coastal zone. Note the reduction in wave power along the western boundary from

a maximum in the south. The wave power distribution along the southern boundary is relatively uniform.

- The orientation of the contours depicts the influence of the dominant south-westerly swell. This is demonstrated by the wave power penetration into False Bay and the calm zone at St Helena Bay.
- Definite wave power concentration zones are found at Cape Point, the entrance of False Bay, Dassen Island and Hangklip.
- The deep-sea wave power resource ranges from 33 to 41 kW/m.

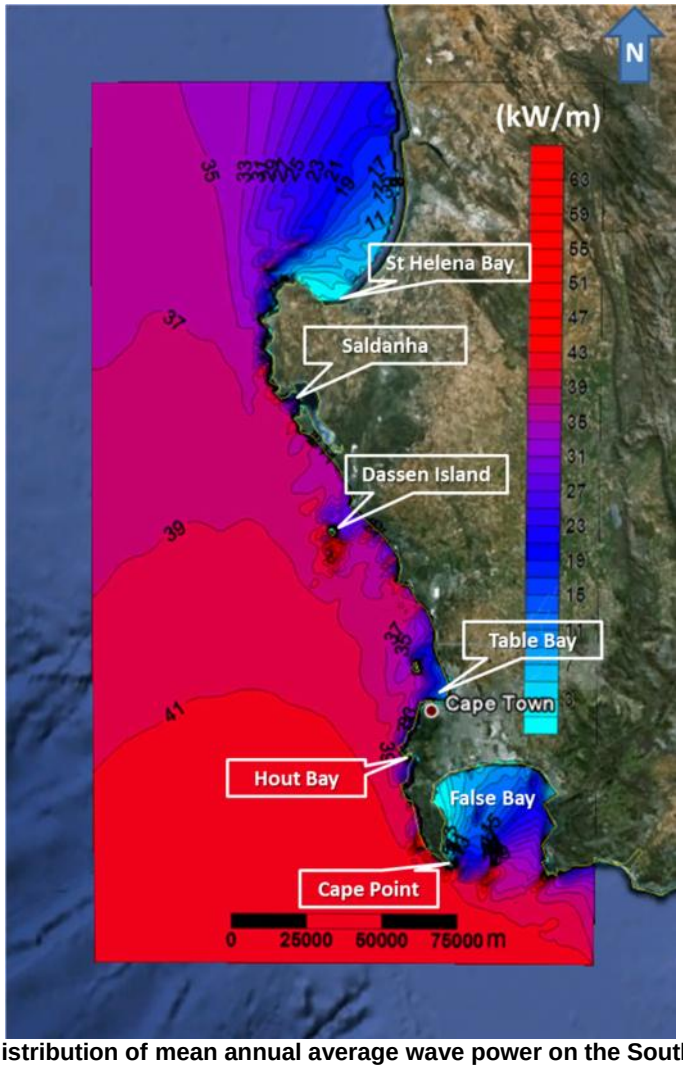

Figure 5-6: Spatial distribution of mean annual average wave power on the South African southwest coast based on 10 years of hindcast wave data

In the next chapter of the report an example case study of a detailed wave power resource assessment for a particular bay on the southwest coast is presented.

6 Spatial distribution of wave power for a specific bay

A detailed resource assessment was conducted for a specific site in Table Bay to determine the electricity generation potential of a breakwater wave energy device to be deployed here. Granger Bay is the proposed deployment location of a wave energy device called the

ShoreSWEC (refer to Joubert (2013)). A wave modelling procedure, similar to that outlined in Chapter 5, was developed to transfer 11 years of offshore hindcast wave data to the site.

6.1 Wave modelling methodology

Similarly to the southwest model, the NCEP wave direction and period data were divided into bins (3 s to 19 s in 1s intervals and 0º to 337.5º in 22.5º intervals) and the average wave height for each combination of direction and period was determined. The average wave height was used instead of a 1 m offshore wave height, as was the case of the southwest model, to provide a better approximation of the general wave height conditions. A SWAN simulation was done for each combination of offshore wave direction, period and its average wave height. The 16 directional and 17 period bins equates to a total of 272 simulations which took approximately 16 hours in parallel sessions on a quad core processor. This wave modelling methodology is schematically presented in Figure 6-1.

6.1.1 Computational and bathymetric grids

A uniform, rectangular computational grid covering an area of 65 km by 140 km was specified for the initial SWAN simulations (refer to "Grid 1" shown in Figure 6-2). Grid 1 has a 250 m by 250 m cell resolution and it was assumed that the offshore NCEP wave conditions apply to each grid point of Grid 1's boundaries. In reality the wave conditions on the boundaries will vary, similar to the southwest coast model, but as waves propagate away from the boundaries, the influence of the seafloor on the wave parameters will rectify this assumption. A second computational grid with a 50 m by 50 m cell resolution was specified a sufficient distance away from the Grid 1 boundaries. SWAN was used to simulate waves from Grid 1's boundaries to the boundaries of Grid 2. Through interpolation SWAN calculated the wave conditions on Grid 2's finer resolution boundary. In order to determine the spatial distribution of wave power at a minimum of 10 grid points along the breakwater structure an even finer resolution computational grid of 10 m by 10 m cells was defined. Figure 6-2 shows the three computational grids used for the wave simulations.

The bathymetric grids were derived from naval charts of the southwest coast and Table Bay (provided courtesy of C. Rossouw).

6.1.2 Boundary conditions

The same boundary conditions were used as discussed in §5.4.2.

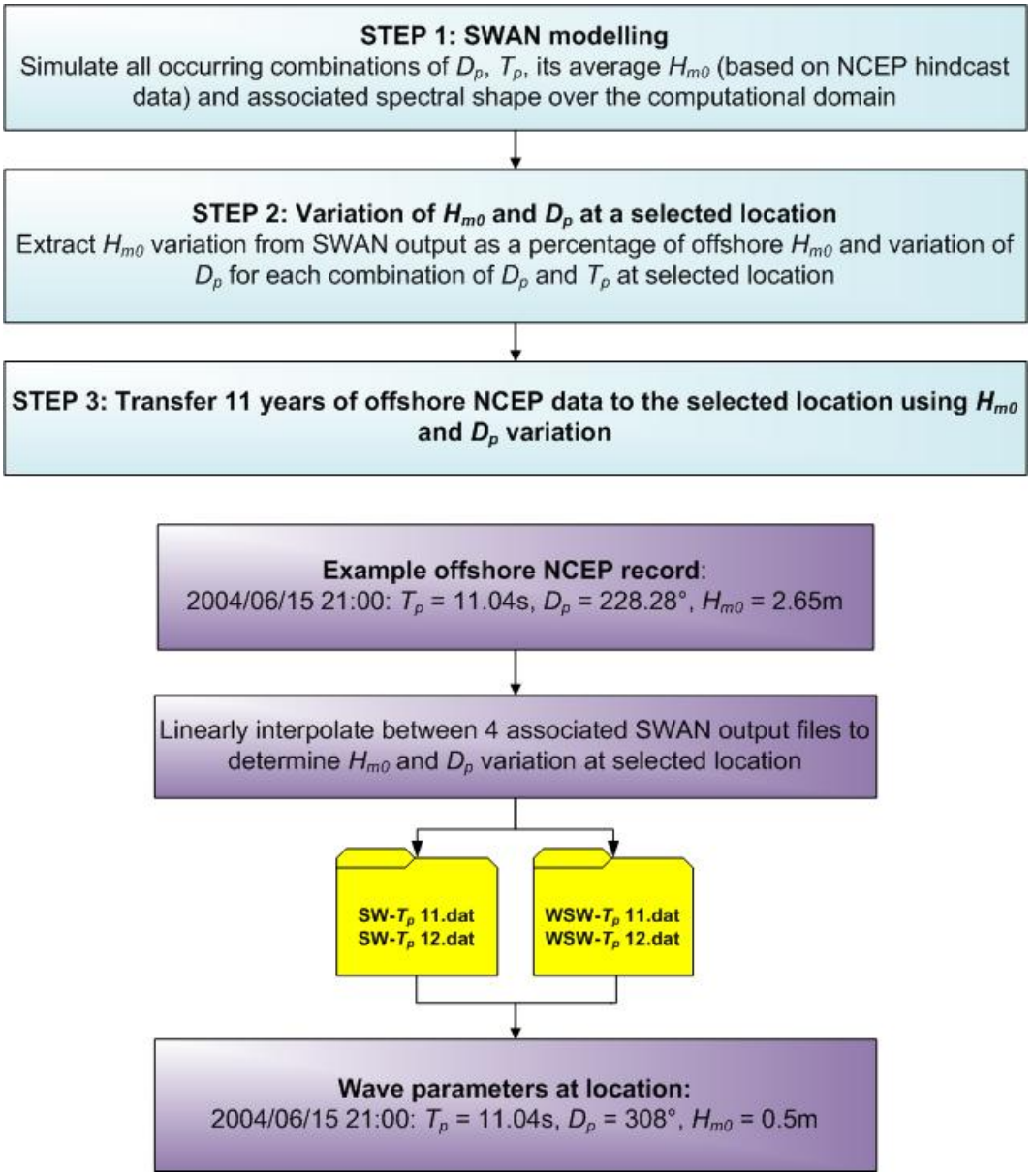

Figure 6-1: Methodology to transfer offshore NCEP hindcast wave data into Table Bay and example output

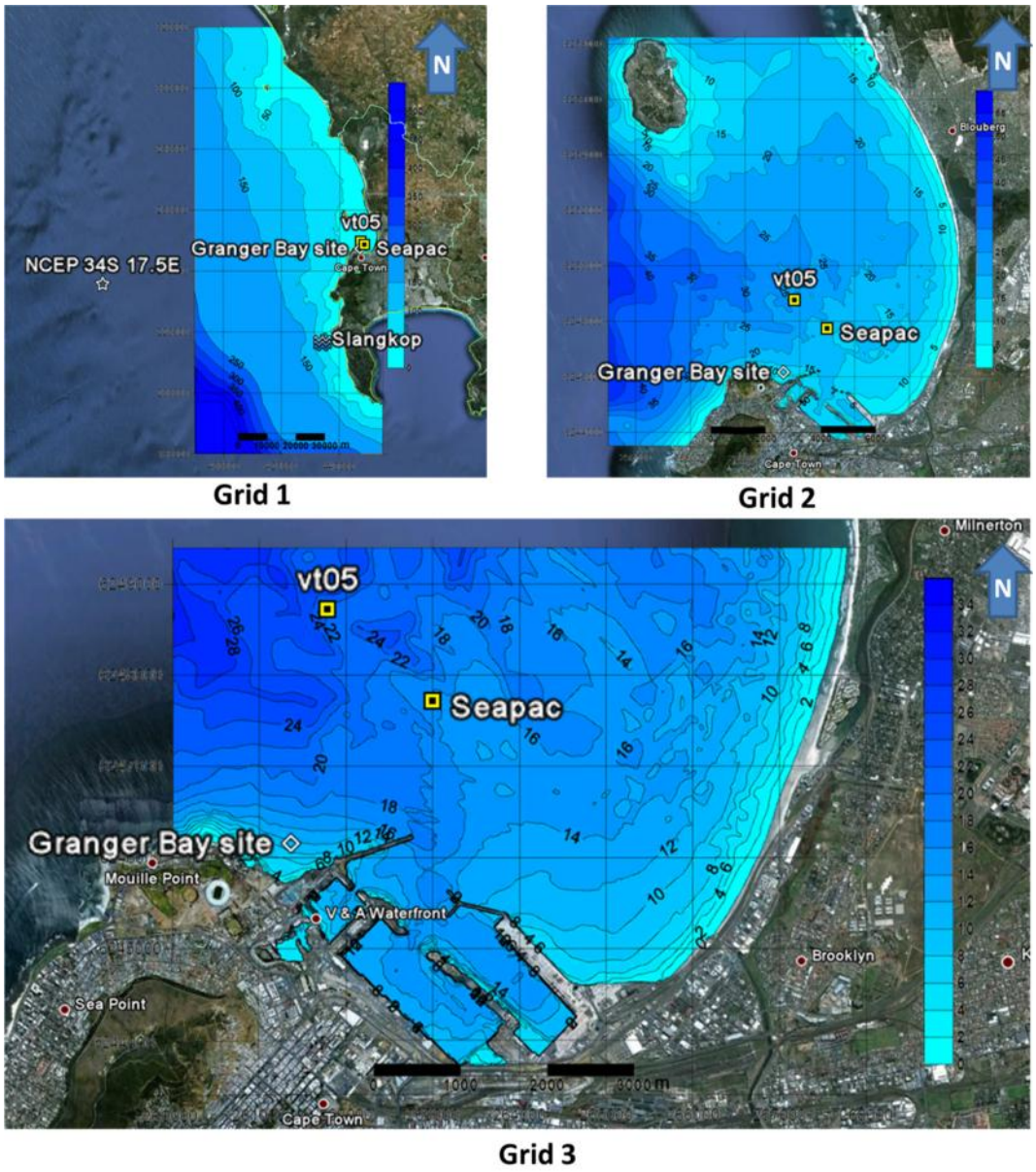

Figure 6-2: Computational and bathymetric grids of Table Bay (water depth in meters below chart datum)

6.2 Table Bay model validation

Rossouw et.al. (2005) developed a real-time wave model for the National Ports Authority of Cape Town to determine wave conditions at selected locations in Table Bay, known as "virtual wave buoys". SWAN was used to simulate waves propagating from Slangkop wave recording station, refer to Figure 6-2 that shows Slangkop's location relative to the NCEP offshore data point and the virtual buoys in Table Bay. Rossouw's model was calibrated with measured data from a Seapac electromagnetic current meter deployed 1.6 km north of the entrance to the Port of Cape Town in 17 m water depth (refer to Figure 6-2). The Seapac was operational for the relatively short period of 1 February to 28 March 2002. The measured Seapac and modelled virtual wave buoy data was made available by National Port Authority to validate the Granger Bay model output.

The measured Seapac wave height data was directly compared to the modelled wave height data. Figure 6-3 shows that the model's values of wave height compares favourably to the Seapac data, but the model does give wave heights which are virtually zero on a few

occasions. Upon closer investigation it was found that the model underestimates the wave height conditions in Table Bay for waves approaching from the southeast to southerly direction. This can be due to the relatively small water area on the model's eastern boundary from which these easterly waves must enter the computational domain.

It is expected to not greatly influence the general wave power resource at Granger Bay, due to the relatively low occurrence of these directional conditions and the small wave height it produces in Table Bay.

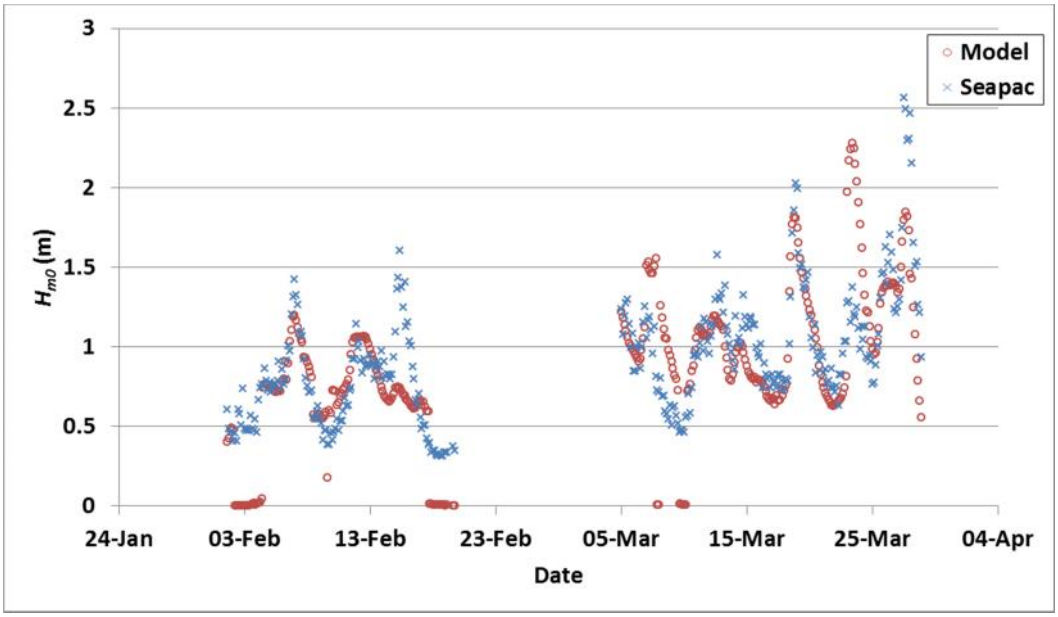

Figure 6-3: Comparison of model and Seapac wave height data of 1 February to 28 March 2002

The correlation between the model and Seapac wave height data was found to have a coefficient of determination, R^2, of 0.55 indicating that 55% of the model wave height data correlates well with the Seapac data over the recording period. This relatively low correlation could be ascribed to the short recording period. Similar correlation analyses with the longer virtual wave buoy data sets (four year overlapping period) showed that the model wave height correlates with 75% of the virtual buoy data (refer to Figure 6-4(b)).

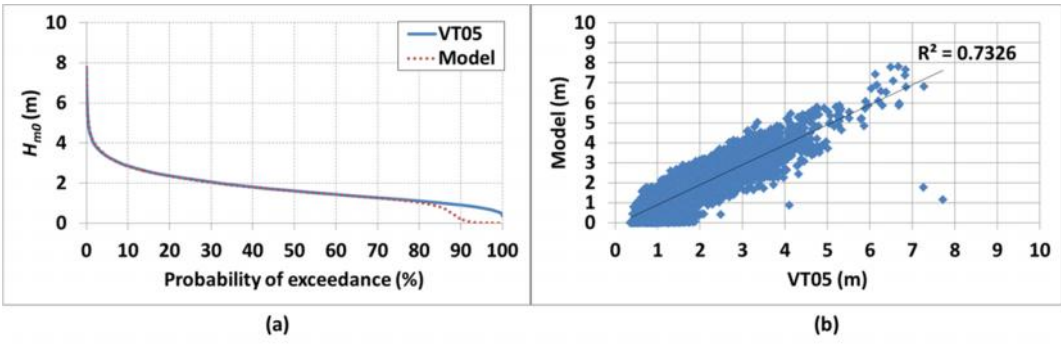

Figure 6-4: (a) Probability of exceedance of model and vt05 wave height data January 2005 to August 2008. (b) Correlation of model and vt05 wave height data

The probability of exceedance curves of the model and Seapac wave heights presented in Figure 6-5 show that the model wave height's probability of exceedance agrees reasonably well with that of Seapac (the exception being the very low values of wave heights from the southeast which were discussed previously). The probability of exceedance of wave height

curves of the model and the virtual buoy data, presented in Figure 6-4(a), compare favourably and have a similar distribution to that shown in Figure 6-5.

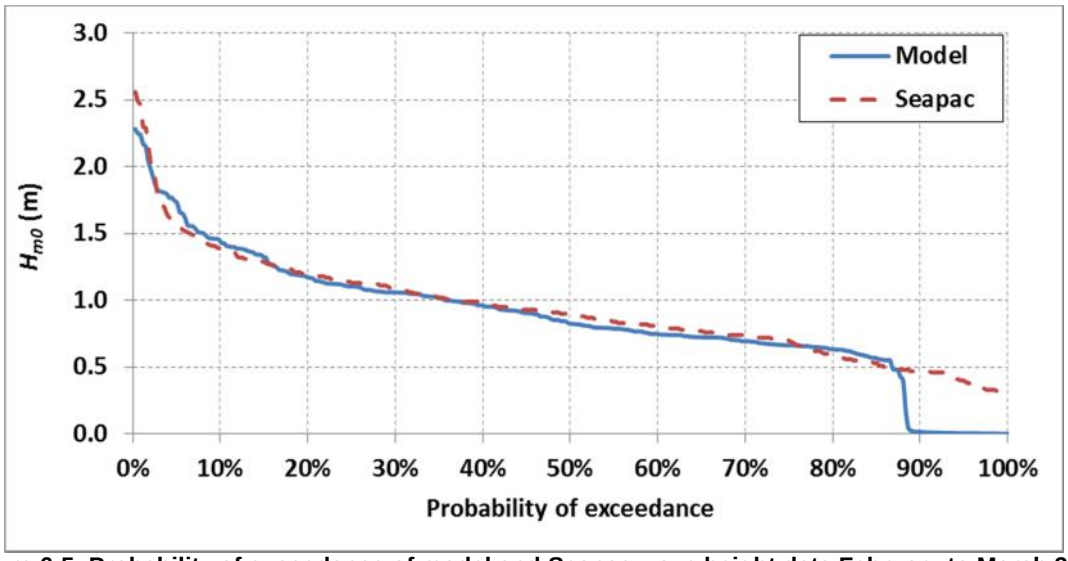

Figure 6-5: Probability of exceedance of model and Seapac wave height data February to March 2002

6.3 Model output

The annual average distribution of wave power in Table Bay based on 11 years of hindcast wave data is presented as a contour map in Figure 6-6. From Figure 6-6 it can be concluded that:

- As would be expected, the greatest wave power resource in Table Bay is on the western boundary and towards the north due to waves penetrating into the bay from the dominant southwest. The port of Cape Town is sheltered from the prevailing wave conditions.
- There is a clear reduction in wave power resource towards the coast due to energy dissipations processes such as bottom-friction.
- A concentration of wave power exists, approximately 2 km south of Robben Island, caused by the 11 m deep reef known as Whale Rock. This may prove to be an ideal location for the deployment of offshore WEC devices and could be a much-needed source of electricity for Robben Island.

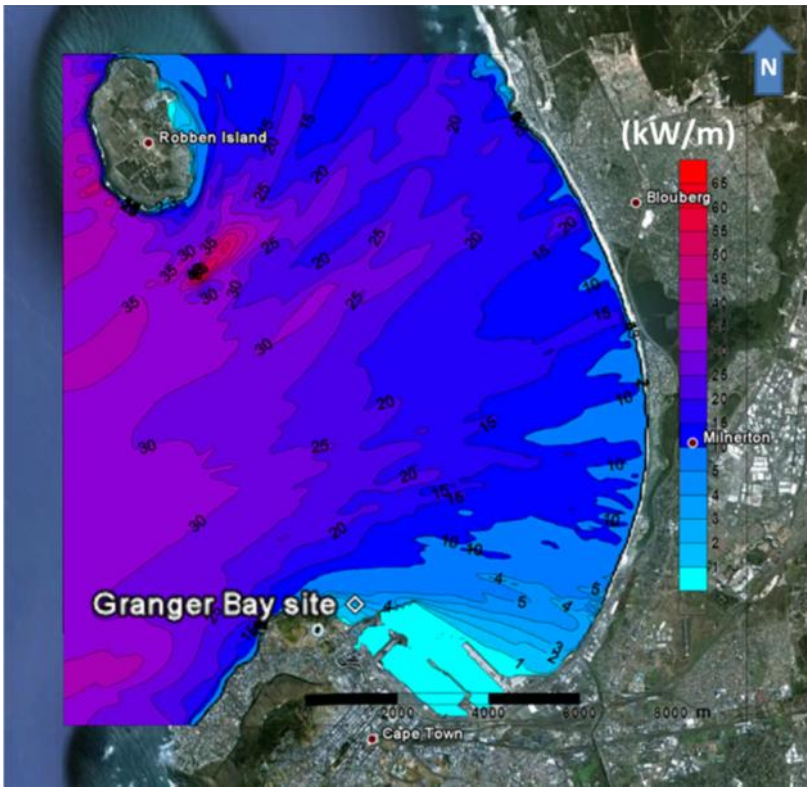

Figure 6-6: Mean annual average wave power distribution (kW/m) of Table Bay based on 11 years of hindcast NCEP wave data

The model can also be used to give a detailed description of the spatial distribution of wave power near-shore as is shown Figure 6-7. This provides helpful information in selecting an exact location for the deployment of a single WEC device or an array of devices.

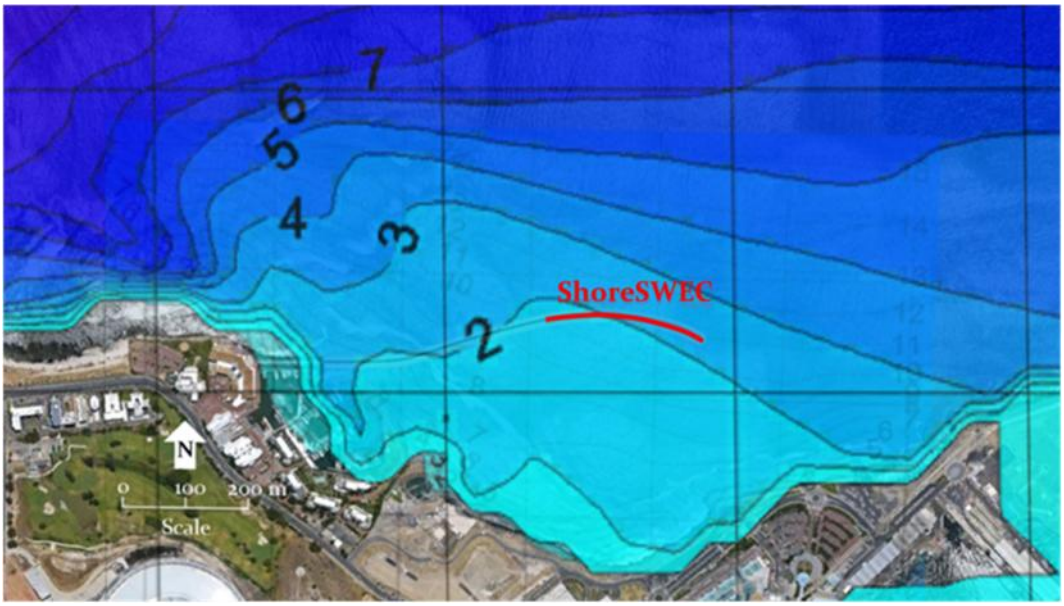

Figure 6-7: Mean annual average wave power distribution (kW/m) at Granger Bay based on 11 years of hindcast NCEP wave data

7 Conclusions and recommendations

The main objective of this report was to provide a detailed description of how to analyse and assess the South African wave power resource by using a specific example. This objective was achieved through measured and numerically modelled wave data analyses. The main findings and conclusions drawn from each section of the report are presented below:

7.1 Measured wave data analysis

- Typical wave height and period conditions are 3 m and 12 s for Slangkop, Cape Point and FA platform, while for Port Nolloth 2 m 12 s waves are the most frequently occurring. Durban has the smallest and shortest waves of 2 m and 9 s.
- The two stations on the southwest coast, Slangkop and Cape Point, have the largest wave power resource based on measured data with a mean annual median value of wave power of approximately 26 kW/m.
- The station with the next greatest resource is FA platform on the south coast with a mean annual median value of wave power of 24 kW/m.
- Port Nolloth on the west coast has a mean annual median value of wave power of 19 kW/m.
- The east coast station of Durban has the lowest wave power with a mean annual median value of approximately 10 kW/m.

7.2 Wave power resource of the southwest coast

A numerical wave modelling procedure was developed to produce maps of the spatial distribution of wave power for the southwest coastal region, the most energetic coastal zone of South Africa. These maps of wave power distribution can be used by device developers to identify locations along the southwest coast best suited for the deployment of their devices. From this analysis it was found that the deep-sea average annual wave power resource ranges from 33 to 41 kW/m.

7.3 Wave power resource of Table Bay

A detailed, high resolution, resource assessment was conducted for Table Bay on the southwest coast as an example case study focussing on Granger Bay as a possible deployment site for a WEC. The generated spatial distribution of wave power illustrated how the prevailing wave conditions penetrate into the bay. A wave power focal zone was identified just north of Robben Island.

7.4 Recommendations

In this study the wave power resource along the South African coast was investigated in detail at specific wave measurement locations. The distribution of wave power off the southwest coastal zone, and in Table Bay specifically, was also assessed in detail. In order to attract more international developers of wave energy devices wave power maps of the entire South African coast is required, similar to what has been done for the UK, Europe, USA, and Australia. The development of these maps requires recorded wave data at various locations of interest along the coast and also digitised bathymetric data. This will bring South Africa one step closer to utilising its abundant wave power resource and becoming a player in this new and exciting energy sector.

8 References

Airy, G. B. 1845. Tides and waves. *Encyclopaedia Metropolitana.* London, Scientific Department, 241 – 396.

Allard, R. Rogers, W.E. 2004. *Validation Test Report for the Simulating Waves Nearshore Model (SWAN): Cycle III, Version 40.11*. Technical report for the Naval Research Laboratory of the United States Navy.

Booij, N. Haagsma, I.J.G. Holthuijsen, L.H. Kieftenburg, A.T.M.M. Ris, R.C. van der Westhuysen, A.J. Zijlema, M. 2009. *SWAN Cycle III version 40.72AB User Manual* Delft University

Carbon Trust. 2005. Marine Energy Challenge: Oscillating water column wave energy converter evaluation report.

CEM. 2006. Coastal Engineering Manual. US Army Corps, Part II Chapter 1: Water wave mechanics.

Cornett, A. M. 2008. A global wave energy resource assessment. *International Offshore and Polar Engineering Conference* paper number 579

Geustyn, L. 1983. Seegolfenergie langs die Suid-Afrikaanse kus: 'n Evaluasie van die tyd en ruimtelike verspreiding. M.Sc thesis, Stellenbosch University. (in Afrikaans).

Goda, Y. 1985. *Random seas and maritime structures*. University of Tokyo Press, Tokyo.

Hagerman, G. Bedard, R. 2003. E2I EPRI specifications: Guidelines for preliminary estimation of power production by offshore wave energy conversion devices.

Heath, T.V. 2011. A review of oscillating water columns. *Philosophical Transaction of the Royal Society A* 370: 235–245.

Holthuijsen L.H. 2007. *Waves in oceanic and coastal waters.* New York: Cambridge University Press.

International Energy Agency, 2011. Key world energy statistics

Joubert, J.R. 2008. *An investigation of the wave energy resource on the South African coast, focusing on the spatial distribution of the southwest coast*. MSc thesis, Stellenbosch University.

Joubert, J.R. 2013. *Design and development of a novel wave energy converter*. PhD dissertation, Stellenbosch University.

MacHutchon K. 2006. *Charaterisation of South African sea storms.* M.Sc thesis, Stellenbosch University.

Mørk, G. Barstow, S. Kabuth A. Pontes M.T. 2010. Assessing the global wave energy potential. *29th International Conference on Ocean, Offshore Mechanics*

and Artic Engineering.

NCEP Internet services team. 2007. *About NCEP*. [Online]. Available: www.ncep.noaa.gov/about/. [2012, November 12].

NOAA: Marine Modeling and Analysis branch. 2012. *WAVEWATCH III® Model*. [Online]. Available: http://polar.ncep.noaa.gov/waves/wavewatch/wavewatch.shtml. [2012, November 12].

Payne G. 2008. *Guidance for the experimental tank testing of wave energy converters*. Technical report written for Supergen Marine.

Pitt, E. G. 2005. Estimating power from wave measurements at the European Marine Energy Centre (EMEC) test site. *Applied Wave Research.*

Retief, G. de F. Prestedge, G.K. Müller, F.P.J. 1982. A proposal for wave energy conversion near Cape Town. *International Conference on Coastal Engineering.* 1: 245 – 260

Rossouw, J. 1989. *Design waves for the South African coastline*. PhD dissertation, Stellenbosch University.

Rossouw, M. Luger, S. Kuipers, J. Patel, S. 2005. Development of a virtual buoy system for the Port of Cape Town, South Africa. *5th International Symposium on Ocean Wave Measurement and Analysis.*

Setoguchi, T. Takao, M. 2006. Current status of self-rectifying air turbines for wave energy conversion. *Energy conversion and management* 47: 2382 – 2396.

Takahashi, S. 1989. Hydrodynamic characteristics of wave-power-extracting caisson breakwater. *21st International Coastal Engineering Conference.* 1 – 3: 2489 – 2501

Van Niekerk, J.L. Retief, G. d. F. 2010. Wave energy converter. Patent IB2009/007682.

Wavegen, 2002, *Islay LIMPET monitoring final report*. Technical report for DTI Sustainable Energy Programmes.